ANNEX

I

Differential responses of global airway, terminal airway, and tissue impedances to histamine

Z. HANTOS, F. PETÁK, Á. ADAMICZA, B. DARÓCZY, AND J. J. FREDBERG
Departments of Medical Informatics and Experimental Surgery, Albert Szent-Györgyi Medical University, H-6720 Szeged, Hungary; and Department of Environmental Health, Harvard School of Public Health, Boston, Massachusetts 02115

Hantos, Z., F. Peták, Á. Adamicza, B. Daróczy, and J. J. Fredberg. Differential responses of global airway, terminal airway, and tissue impedances to histamine. *J. Appl. Physiol.* 79(5): 1440–1448, 1995.—The forced oscillation and alveolar capsule techniques were applied to determine the input impedance of the lungs and the airway transfer impedances between 0.2 and 20 Hz in six open-chest dogs in the control state, during intravenous infusion of histamine at seven rates between 0.25 and 16 $\mu g \cdot kg^{-1} \cdot min^{-1}$, and after the infusion. In each condition, the input impedances seen from the alveolar capsules, i.e., terminal airway impedance (Zaw,ter), were measured by imposing 2- to 200-Hz oscillations from the capsules (B. L. K. Davey and J. H. T. Bates. *Respir. Physiol.* 91: 165–182, 1993). Airway resistance (Raw) and inertance and tissue damping and elastance were derived from the lung impedance data. For all dogs, histamine progressively increased Raw and the real part of airway transfer impedance (airway transfer resistance), reaching, at 16 $\mu g \cdot kg^{-1} \cdot min^{-1}$, 241 ± 109 (SD) and 370 ± 186%, respectively, of the control values, but caused greater, although locally highly variable, increases (769 ± 716% of the control value) in the real part of Zaw,ter extrapolated to zero frequency (R0). With increasing doses of histamine, the changes in R0 always preceded those in Raw and airway transfer resistance implying that bronchoconstriction developed first in the lung periphery. It is therefore concluded that the measurement of Zaw,ter offers a sensitive method for the detection of early nonuniform responses to bronchoconstrictor stimuli that are not yet reflected by the values of the overall Raw. In one-half of the cases, significant increases in tissue damping and elastance occurred before any change in R0; this suggests that the mechanisms of airway and parenchymal constrictions may be unrelated.

airway resistance; lung tissue elastance; lung tissue resistance; peripheral airways; bronchoconstriction; tissue constriction; forced oscillations

IT HAS BEEN WELL DOCUMENTED that bronchoactive substances have marked effects on mechanical properties of the lung parenchyma as well as of the pulmonary airways (2, 3, 15–25, 27–28, 30). Recent reports by Mitzner et al. (24) and Lauzon et al. (17) have presented evidence that the primary locus of changes in parenchymal mechanical properties during agonist challenge is, in fact, constriction of the intraparenchymal airway, which is tethered to the parenchyma by an airway-parenchymal elastic interdependence. Lauzon et al. (17) and Bates and Peslin (3) also suggested that constriction of the smooth muscle elements in the walls of the peripheral bronchi and blood vessels is responsible for the changes in the parenchymal elastance and that the airway resistance (Raw) is altered mainly via the constriction of more central airways. These findings suggest that stimulation of intraparenchymal contractile cells need not be invoked to explain most of the observed changes in parenchymal mechanics. Rather, bronchial smooth muscle is functionally a part of the lung tissue and accounts for most of the parenchymal response.

In this report, we examined in some detail the notion that bronchospasm accounts for the greater part of the parenchymal response. We have used three independent measures of airway caliber. First, we estimated the overall airway impedance from pulmonary impedance data measured with forced oscillations at the airway opening (14, 15). Second, we obtained direct measures of the airway transfer impedance (Zaw,t) using alveolar capsules (12). Third, we adapted the capsule oscillation method of Davey and Bates (8) to determine the terminal airway impedance (Zaw,ter), which is a sensitive assay of small-airway caliber. We found that the most responsive indicator of the changes in lung resistance (RL) was always Zaw,ter, but its dose-dependent changes were often preceded by those in the tissue impedance. Thus, we conclude that small-airway bronchospasm does not uniquely account for contractile responses of lung parenchyma.

METHODS

Animal preparation. Six mongrel dogs weighing 23.2 ± 2.6 kg were studied in the supine position. The animals were anesthetized with pentobarbital sodium (30 mg/kg initial dose, supplemented hourly with a 10 mg/kg dose), and a catheter was introduced into a femoral artery for monitoring systemic arterial blood pressure. A tracheotomy was performed, and a 15-mm-ID metal tube was inserted into the distal trachea. The dogs were paralyzed with an initial dose of 0.1 mg/kg of pipecuronium bromide, supplemented with 0.05 mg/kg doses every 2 h. A thoracotomy was accomplished with bilateral incisions between the fifth and sixth ribs and transverse splitting of the sternum. Mechanical ventilation was maintained with a Harvard respirator at frequencies of 12–15 breaths/min and a tidal volume of 20 ml/kg, with 5-cmH_2O positive end-expiratory pressure.

Tracheal oscillations. The input impedance of the lungs (ZL), the tissue transfer impedance (Zti,t), and airway transfer impedance (Zaw,t) were determined from the measurement of transpulmonary pressure, tracheal airflow ($\dot{V}$), and local alveolar pressure (PA) during small-amplitude volume oscillations imposed in the central airway with a technique similar to that previously described in detail (15). In short, a computer-controlled volume generator (a closed-box loudspeaker system) produced pseudorandom volume oscillations of <40 ml peak to peak at the airway opening containing noninteger-multiple frequency components (6) in the range of 0.2–21.1 Hz with optimized phase angles to attain the minimum amplitude of the composite signal (7). $\dot{V}$ was measured with a 28-mm-ID heated screen pneumotachograph

and a Validyne MP-45 (±2 cmH_2O) transducer. Airway opening pressure was measured with another MP-45 (±30 cmH_2O) sensor via a side tap of the tracheal tube. Measurement of PA was made by means of Plexiglas alveolar capsules devised specifically to allow multiple transpleural punctures to be performed in small separate pleural areas (26) and affixed to relatively flat lobar surfaces with cyanoacrylate glue (Pattex, Henkel, Germany). The bottom plate of the capsule chamber was 2.5 mm thick and contained four 1-mm bores across which the visceral pleura was punctured to a depth of 1 mm with a conical pin of 0.8-mm maximum diameter. When bleeding or oozing from the lung was observed, the puncture was blocked by injecting a small amount of Vaseline into the corresponding bore, and a new puncture was made through one of the other bores until two dry connections communicating well with the subpleural alveolar regions were established in each of the five capsules. Wherever this was not successful, the whole capsule was plugged, and, if sufficient surface area was available on the lung, a new capsule was affixed to replace the plugged one. Eventually, stable recordings of PA were obtained in five capsules in three dogs, in four capsules in two dogs, and in three capsules in one dog; these capsules were placed on two to four lobes within each animal. The capsule chamber was connected to a 12-mm 2-mm-ID metal tube with a 1-mm-ID sidearm where the capsule pressure was measured with an ICS model 33NA002D miniature transducer. The other end of the metal tube was connected to the wave tube through a short segment of thin-walled Silastic tubing, which was clamped by a light crocodile clip during tracheal oscillations. The whole capsule assembly was suspended with the transducer cable and wave tube so that the load on and the deformation of the lung surface were minimal.

Capsule oscillations. The Zaw,ter was measured by the wave-tube technique (12, 31). Twenty-eight-centimeter pieces of polyethylene catheter (0.062 in. ID) served as wave tubes; they were connected to the front chamber of a small loudspeaker-in-box system containing a 40-mm-diam headphone speaker and ended in the Silastic tube segment of each capsule assembly, which was opened by removal of the crocodile clip. Under the circumstances of the relatively high load impedance, the loudspeaker system acted as a pressure generator, and it was driven by a noninteger-multiple pseudorandom signal with 46 components between 2 and 200 Hz and a repetition time of 4 s. The pressure excursion in the front chamber, i.e., at the catheter inlet (Pin), measured with an ICS model 33NA002D transducer, was within ±0.3 cmH_2O, whereas the outlet pressures ($P_{out} \approx PA$) ranged between ±0.14 and ±0.3 cmH_2O, depending on the value of the actual load impedance on the catheter (Zm). The latter was calculated as

$$Zm = [Z_0 \sinh(\gamma l)]/[TF - \cosh(\gamma l)]$$

where Z_0, γ, and l are the characteristic impedance, the complex propagation wave number, and the length of the catheter, respectively, and TF is the pressure transfer function, i.e., the ratio of P_{out} to P_{in}. Z_0 and γ can be expressed as

$$Z_0 = (Z/Y)^{1/2}$$

$$\gamma = (ZY)^{1/2}$$

where Z and Y are the series impedance and the shunt admittance per unit length of the tube, respectively (12, 31). Their values, as functions of frequency, were computed on the basis of geometric data and material constants determining the frictional and mass effects of the oscillating air in the catheter (series impedance) and the compressibility of air and the thermal conductivity of the catheter wall (shunt admittance), according to Franken et al. (9).

In model experiments, we measured the impedance of the capsule assembly alone (Z'm) as part of the load impedance on the wave tube by leaving two holes in the baseplate open to the atmosphere and sealing the other holes with pieces of adhesive tape. In this way, we determined the impedance of the pathway between the sidearm of the outlet pressure sensor and the bottom surface of the capsule. The Z'm values were fairly independent of the oscillation amplitude in the range of flows recorded during the measurements of Zm and were consistent with the impedance data calculated from the capsule geometry: the real part of Z'm increased from 21 to 34 $cmH_2O \cdot s \cdot l^{-1}$ between 2 and 200 Hz, and the imaginary part of Z'm was consistent with an inertance value decreasing from 0.12 to 0.10 $cmH_2O \cdot s^2 \cdot l^{-1}$ between 2 and 200 Hz. Z'm was regarded as an in-series component of Zm, and it was subtracted from all Zm data to obtain Zaw,ter. A rough estimate of the resistance of the transpleural punctures was also obtained by sealing all holes and puncturing the tapes on two holes with approximately the same diameters as those made across the pleura. Five capsules were prepared in this way, and their impedances were measured. After the subtraction of Z'm from these impedances, frequency-independent real parts ranging from 70 to 220 $cmH_2O \cdot s^{-1} \cdot l^{-1}$ and negligibly small inertive imaginary parts were found. These incidental modeled values were not subtracted from the Zaw,ter data.

Protocol. The measurements were made in the control state, during intravenous infusion of histamine in seven steps beginning with a rate of 0.25 $\mu g \cdot kg^{-1} \cdot min^{-1}$ (*H1*) and subsequent doubling up to 16 $\mu g \cdot kg^{-1} \cdot min^{-1}$ (*H2* through *H7*), and 60 min after the last infusion. The durations of a tracheal and a capsule oscillation were 20 and 4 s, respectively. In both the control state and postinfusion, four measurements were made with tracheal oscillation, the capsules were then oscillated six times, and the results from the repeated measurements were ensemble averaged. In *H1* through *H7*, capsule oscillations were performed every 2 min after the onset of the infusion until the TF values plateaued for three consecutive measurements. This was followed by four tracheal oscillations, and three capsule oscillations were again recorded. The recordings of the six tracheal and four capsule oscillations during the plateau were ensemble averaged. After each oscillatory measurement, the mechanical ventilation was resumed starting with a moderate hyperinflation accomplished by closing the expiratory outlet of the respirator for one respiratory cycle. The time elapsed between every two consecutive measurements was 2 min. Immediately before the oscillations, the respirator was detached at end expiration from the tracheal cannula, which was either connected to the loudspeaker chamber preinflated to 5 cmH_2O (tracheal oscillation) or clamped (capsule oscillation).

Computations. The cross-power spectra (G_{xU}) between the driving signal (U) and every measured signal (x) were computed by fast Fourier transformation, and ZL, Zti,t, and TF were obtained as $ZL = G_{P_{aw}U}/G_{\dot{V}U}$, $Zti,t = G_{P_{aw}U}/G_{\dot{V}U}$, and $TF = G_{P_{out}U}/G_{P_{in}U}$. Zaw,t was calculated as Zaw,t = ZL − Zti,t, and Zaw,ter was derived from TF and Z'm as described above.

The ZL data between 0.2 and 4.9 Hz were evaluated in terms of a model containing Raw, airway inertance (Iaw), and a constant-phase tissue compartment in which the real and imaginary parts decrease with the same power (α) of angular frequency (ω)

$$ZL = Raw + j\omega Iaw + (G - jH)/\omega^{\alpha} \quad (1)$$

where j is the imaginary unit and G and H are coefficients of tissue damping and elastance, respectively (15). This model

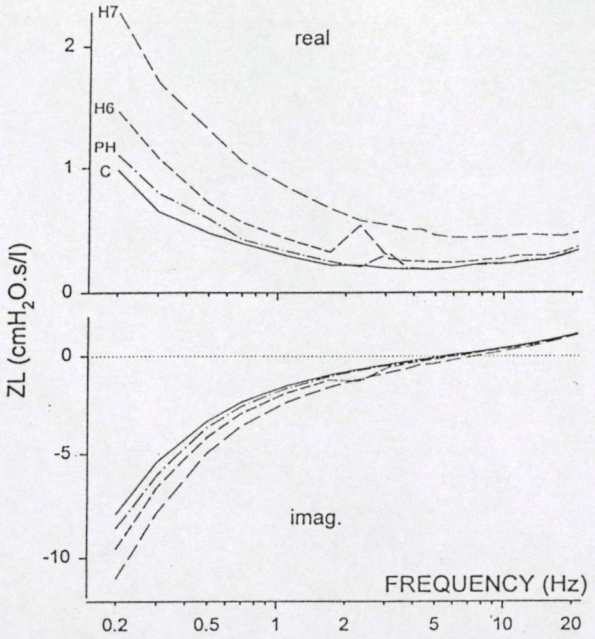

FIG. 1. Pulmonary input impedance (ZL) in control state (C), during infusion of histamine at rates of 8 (*H6*) and 16 $\mu g \cdot kg^{-1} \cdot min^{-1}$ (*H7*), and 60 min postinfusion (PH) in *dog 1*. Values are means from 4 successive measurements in each condition. imag., Imaginary.

was also formally applied to determine the values of the tissue transfer damping (Gt) and elastance (Ht) in a subset of Zti,t measurements. The Zaw,ter data were fitted by a simple model consisting of a resistance (R_1) in series with a parallel resistance (R_2) – compliance (C) unit

$$Zaw,ter = R_1 + (R_2/j\omega C)/[R_2 + (1/j\omega C)] \quad (2)$$

The impedance functions described by *Eqs. 1* and *2* were fitted to the measured data with a global optimization procedure (5). In the case of the ZL data, unique parameter sets were obtained, whereas only some of the Zaw,ter data had a frequency dependence characteristic enough to provide stable estimates for R_1, R_2 and C. This problem, as referred to later and detailed in APPENDIX, restricted the evaluation of the Zaw,ter data in terms of zero frequency resistance $R0 = R_1 + R_2$.

The results of the transfer impedance measurements were characterized by the average values of the real part of Zaw,t [airway transfer resistance (Raw,t)] in the range of 0.2–4.9 Hz. Any model-based evaluation of the Zaw,t data was precluded by the fact that the transfer impedance was defined here for a single-input multiple-output system in which the input quantities (airway opening pressure and $\dot{V}$) and one output quantity in each capsule (PA) were measured. We also note that the averaging of Raw,t data was correct only when they were independent of a frequency < 5 Hz. In some cases at high infusion rates, marked falls in Raw,t with frequency increasing from 0.2 Hz were observed; the ambiguity in the interpretation of such Raw,t data will be indicated in the RESULTS and discussed thereafter.

The statistical significance of changes in the pulmonary mechanical parameters was evaluated by using Wilcoxon's signed-rank test.

RESULTS

An example of the ZL vs. frequency data under different experimental conditions is presented in Fig. 1. For clarity, data from the control and postinfusion states and three infusion rates are included. Histamine caused progressive increases in the real part of ZL [lung resistance (RL)], which were higher at low frequencies where elevations in both tissue resistance and Raw are reflected and smaller at higher frequencies where Raw dominates. The relative changes in the magnitude of the low-frequency imaginary part of ZL were similar to but somewhat smaller than those of RL. The postinfusion data were in general between those in the control and the higher rate infusions.

In the vast majority of cases, the Raw,t values were independent of frequency up to 7–8 Hz (the difference between the maximum and minimum values was

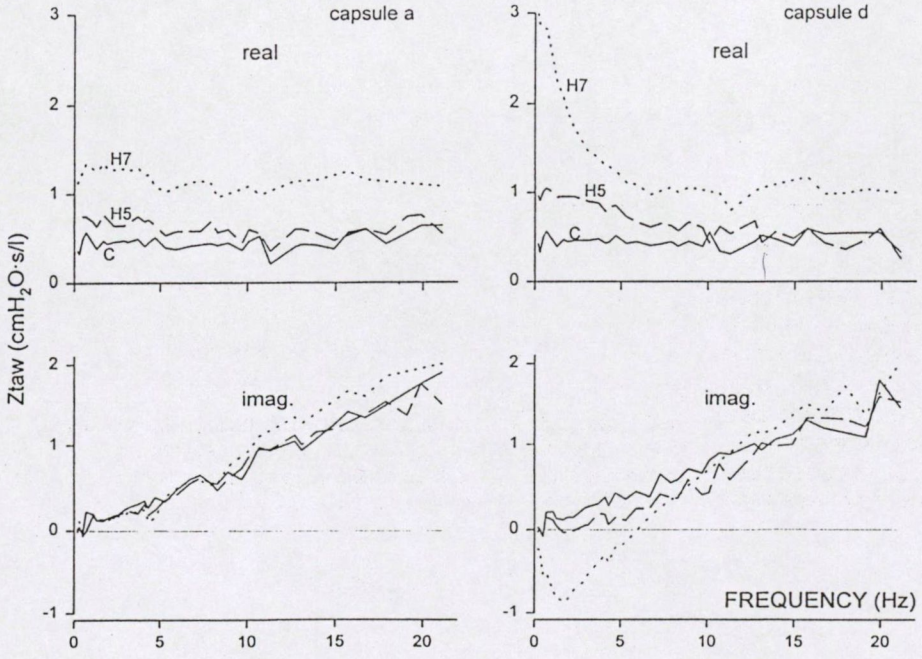

FIG. 2. Airway transfer impedance (Zaw,t) estimated from 2 capsules in *dog 5* in control state and during infusion of histamine at rates of 4 (*H5*) and 16 $\mu g \cdot kg^{-1} \cdot min^{-1}$ (*H7*). Values are means from 4 successive measurements in each condition.

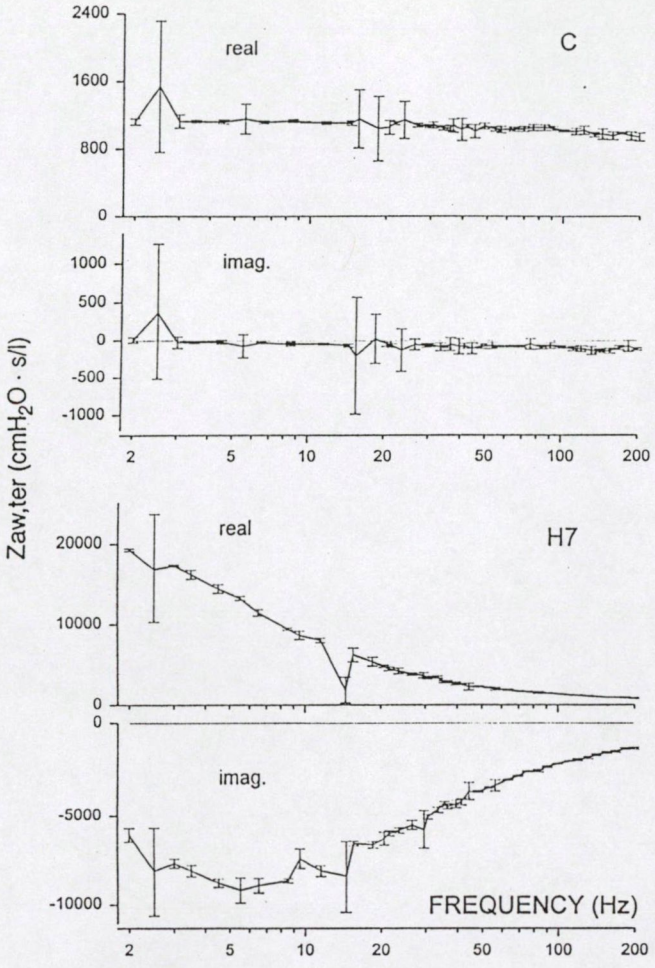

FIG. 3. Terminal airway impedance (Zaw,ter) in control state and during infusion of histamine at 16 $\mu g \cdot kg^{-1} \cdot min^{-1}$ in 1 capsule in *dog 2*. Values are means ± SD from 6 measurements in each condition.

<20% up to 4.9 Hz) and the imaginary parts of Zaw,t (airway transfer reactance) increased linearly with frequency in all experimental conditions (Fig. 2, *capsule a*). However, Raw,t showed a marked negative-frequency dependence at *H7* in two of the five capsules in *dog 1* and at *H6* and *H7* in two of the four capsules in *dog 5* where these patterns were accompanied by airway transfer reactance values departing from the linear increase. Such an exceptional Zaw,t is illustrated in Fig. 2, *capsule d*, indicating that the zero-frequency Raw,t was seriously underestimated by the mean Raw,t value in these cases.

In Fig. 3, two examples are given of the Zaw,ter vs. frequency data. When Zaw,ter was low in magnitude, it appeared as a rule almost purely resistive: the terminal airway resistance values were fairly constant and declined slightly only in the highest frequency region, and the terminal airway reactance values showed mild decreases with increasing frequency. Once the infusion of histamine led to substantial increases in Zaw,ter, a sigmoid-shaped negative-frequency dependence of terminal airway resistance developed, and the augmented fall in terminal airway reactance was followed by a reversal at higher frequencies.

The dose-dependent changes in the pulmonary mechanical parameters were highly variable among the dogs. Increases in the G and H occurred at *H1* in some animals but usually only at higher doses. For all dogs (Table 1), the mean value of G became significantly different from the control state at *H3* and reached its maximum at *H7* (236 ± 60% of the control value). The changes in H were milder: the maximum was 136 ± 11% of the control value at *H7* and the differences from the control value became statistically significant at *H4*. As a consequence of these changes, the tissue hysteresivity (13), i.e., η = G/H, at *H3* was significantly higher than the control value and reached 169 ± 40% of it at *H7*. All of these tissue parameters remained elevated after the infusion. The G values normalized by the control data are plotted against the normalized H values for each dog in Fig. 4. This again shows that the increases in G were disproportionately higher than those in H, and, remarkably, the deviations from the line of identity (η is constant) occurred even on the initial small changes in these parameters. We note also that the postinfusion G and H values were situated around those at the medium-rate infusions of histamine.

The changes in airway parameters reflected the responsiveness to histamine differently. In some animals, the Raw,t values were fairly uniform among the capsules, and R0 normalized by the corresponding value in the control state ($R0_{Cont}$) exhibited closely similar dose dependences, whereas in other animals there

TABLE 1. *Pulmonary mechanical parameters*

	Raw	Iaw	G	H	η	Raw, t	R0
Cont	0.241±0.142	0.0118±0.0019	1.41±0.33	12.44±2.68	0.113±0.013	0.220±0.141	3,142±2,631
H1	0.241±0.132	0.0114±0.0016	1.45±0.45	12.57±2.88	0.115±0.018	0.218±0.128	3,238±2,666
H2	0.238±0.132	0.0117±0.0020	1.65±0.57	13.00±3.49	0.125±0.017	0.223±0.132	3,893±3,082
H3	0.240±0.136	0.0118±0.0019	1.93±0.76*	13.83±4.15	0.138±0.021*	0.246±0.153	5,218±5,317
H4	0.260±0.148	0.0117±0.0017	2.17±0.84*	15.06±4.52*	0.142±0.024*	0.281±0.194*	7,303±8.679*
H5	0.284±0.178	0.0116±0.0017	2.43±0.82*	15.65±4.38*	0.153±0.022*	0.351±0.282*	10,275±13,574*
H6	0.386±0.270	0.0116±0.0019	2.74±0.85*	16.57±4.30*	0.164±0.022*	0.518±0.459*	14,656±16,459*
H7	0.597±0.431*	0.0113±0.0025	3.23±0.93*	17.13±4.14*	0.188±0.026*	0.865±0.685*	21,801±20,094*
PH	0.234±0.116	0.0122±0.0019*	1.91±0.54*	14.09±3.14*	0.134±0.016*	0.260±0.151	3,422±2,455

Values are means ± SD; n = 6 dogs. Raw, airway resistance (in $cmH_2O \cdot s \cdot l^{-1}$); Iaw, airway inertance (in $cmH_2O \cdot s^2 \cdot l^{-1}$); G, tissue damping (in cmH_2O/l); H, tissue elastance (in cmH_2O/l) (all calculated from model fitting to input impedance data); η, tissue hysteresivity (η = G/H); Raw,t, airway transfer resistance (in $cmH_2O \cdot s \cdot l^{-1}$); R0, terminal airway resistance extrapolated to zero frequency (in $cmH_2O \cdot s \cdot l^{-1}$), cont, control state; *H1–H7*, histamine infusion steps with doubling of rate from 0.25 (*H1*) to 16 $\mu g \cdot kg^{-1} \cdot min^{-1}$ (*H7*); PH, 1 h postinfusion. * Significantly different from control value.

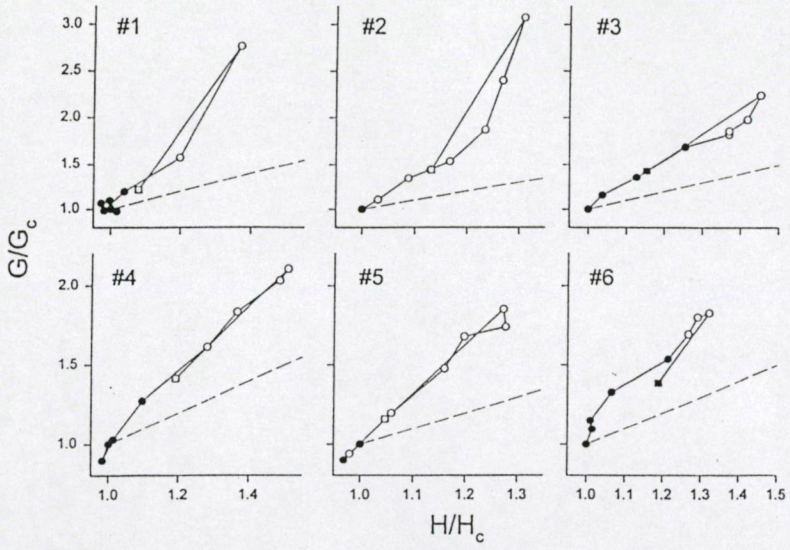

FIG. 4. Relationship between tissue damping (G) and elastance (H), both normalized by control values (G_c and H_c), in control state, at increasing rates of histamine infusion (circles) and 60 min postinfusion (squares) in each dog (nos. at *top left*). Filled symbols, conditions in which terminal airway resistance did not exceed control value in any capsule; dashed lines, lines of identity corresponding to constant hysteresivity.

were marked local differences in Raw,t and R0/R0$_{Cont}$, occasionally with different patterns of dose dependence in the latter. Examples of both uniform and nonuniform regional responses are given in Fig. 5. In *dog 1*, both Raw,t and R0 showed huge regional differences in the peak response, whereas in *dog 2* the initial dissociation of the R0/R0$_{Cont}$ curves was followed by a more uniform regional behavior at the higher doses. For all dogs (Table 1), the statistically significant elevations from the control levels occurred at *H7*, *H4*, and *H4*, and the responses at *H7* were 241 ± 109, 370 ± 186, and 769 ± 716% of the control values for Raw, Raw,t, and R0, respectively. In none of these parameters were the postinfusion values significantly different from the control ones. The values of R0 were characterized by great interindividual differences (the range of the pooled data was from 244 to 8,008 $cmH_2O \cdot s \cdot l^{-1}$) and considerable intraindividual differences (from 103 to 745% of the lowest R0 value in a given dog) in the control state. Because of the different number of capsules in the dogs, the mean values for all animals (Table 1) were obtained by taking the average Raw,t and R0 for each dog. Nevertheless, we wondered whether the changes in R0 depend on the baseline value (R0$_{Cont}$) and calculated the regression between the maximum R0 (R0$_{max}$), normalized by the corresponding R0$_{Cont}$ value (R0$_{max}$/R0$_{Cont}$), and R0$_{Cont}$. Although the regression predicted a slight positive dependence of R0$_{max}$/R0$_{Cont}$ on R0$_{Cont}$, the correlation coefficient was low (r = 0.40). Comparison of the Raw,t and R0 data with respect to the placement of capsules did not show statistically significant differences between the values ob-

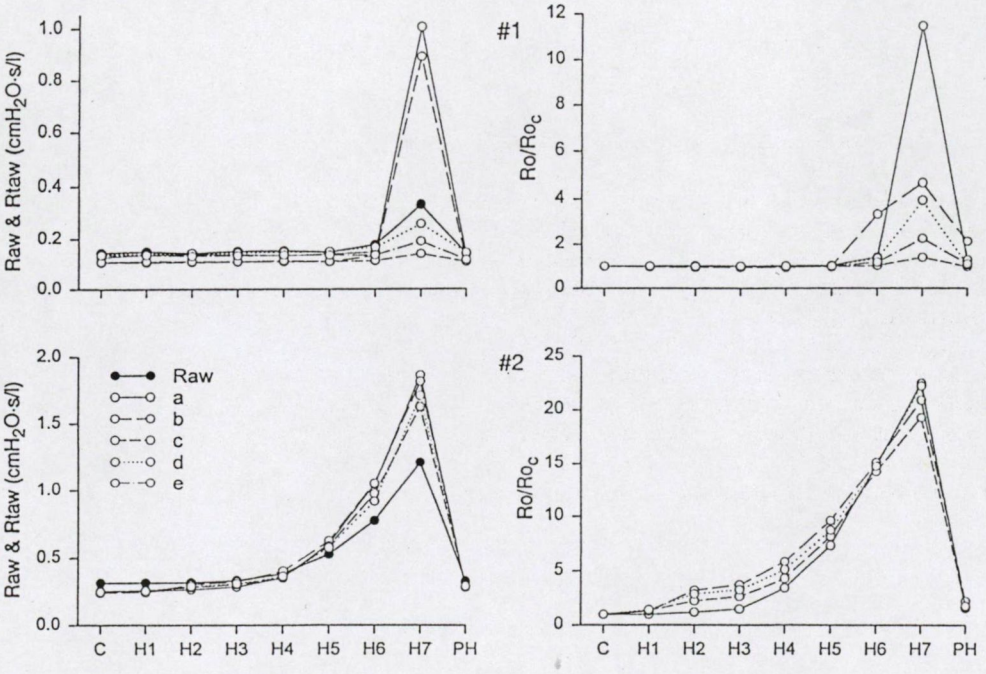

FIG. 5. Airway parameters in control state, during infusion of histamine at rates doubling from 0.25 (*H1*) to 16 $\mu g \cdot kg^{-1} \cdot min^{-1}$ (*H7*), and 60 min after infusion in *dogs 1* and *2*. *Left*: airway resistance (Raw) and transfer airway resistance (Raw,t) in *capsules a–e*. *Right*: terminal airway resistances extrapolated to zero frequency and normalized by control value (R0/R0$_c$) in the same capsules.

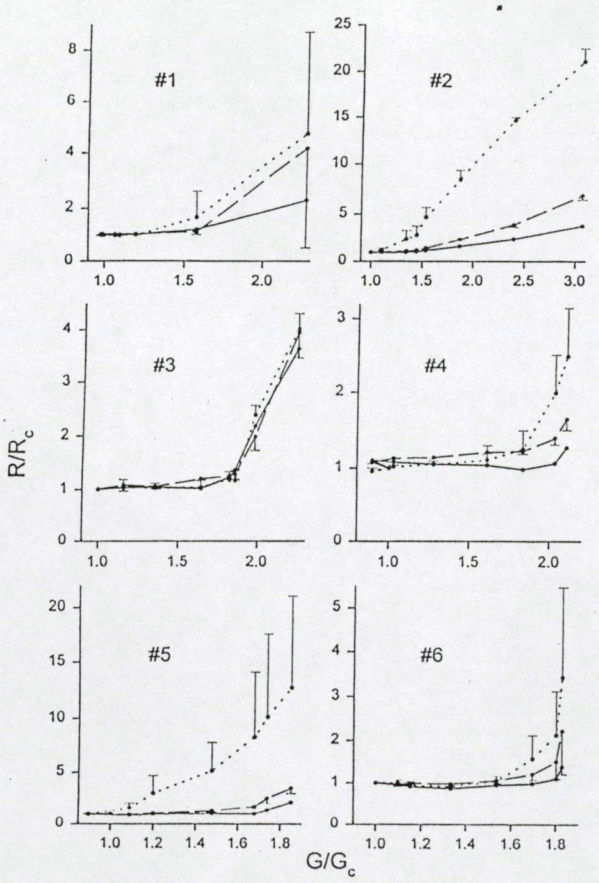

FIG. 6. Airway resistance (R) vs. tissue damping (G), normalized by control values, in each animal (no. in each graph). Data include control state and during 7 rates of histamine infusion. Solid line, Raw; dashed line, Raw,t; dotted line: R0. For Raw,t and R0, values are means ± SD from all capsules.

tained in different lobes. Airway inertance changed by less than ±5% throughout the experiment, and the statistically significant differences from the control level, occurring incidentally at *H1* and postinfusion, are inconclusive. We note that the mean values and the significance of differences from the control values (Table 1) are tentative with regard to all parameters because widely different individual dose-response patterns were averaged.

Raw, Raw,t, and R0 are plotted against G for each dog in Fig. 6, with all parameters normalized by their control values. In all dogs but one (*dog 3*), where all airway parameters ran fairly together, the highest and earliest dose-dependent changes were exhibited by R0, whereas Raw turned out to be far less responsive. The increases in Raw,t were generally between those in Raw and R0. This representation of data also makes it clear that considerable elevations in G may occur without any change in Raw; in addition, in three dogs (*dogs 3, 4,* and *6*) the increases in G by from 55 to 85% were not accompanied by significant changes in any of the airway parameters including the individual values of the most sensitive R0.

The G and H values were compared with the corresponding Gt and Ht values in the subset of measurements where the most sensitive airway parameter (R0) changed by <10% of the control levels in each dog. Both the G vs. Gt and the H vs. Ht data fell close to the line of identity and showed high correlations ($r > 0.92$ and $r > 0.98$, respectively).

DISCUSSION

Loring et al. (18) demonstrated that the viscous resistance of lung tissue (Rti) comprised a significant proportion of RL at the frequency of spontaneous breathing and that histamine challenge caused increases in both Raw and Rti. This finding has been confirmed in a number of studies (1, 3, 11, 15, 17, 19, 21–25, 27, 28, 30), although the observations regarding the relative contributions of the airways and the tissues to the increase in RL and their dose dependences were different. Ludwig et al. (22) found that at submaximal doses of inhaled histamine the sensitivity of the airways was similar to that of the tissues in open-chest dogs, whereas at the lobar level a marked disparity was observed between the airway and tissue responses (21). In the young dogs studied by Sly and Lanteri (30), the elevations in Rti with increasing doses of histamine were accompanied uniformly by relatively small and lagged increases in Raw, and similar patterns of response were also observed by Romero and Ludwig (27) and Romero et al. (28) in rabbit lungs in which tissue constrictions were evoked by methacholine. Although from incidental parallel changes in Raw and Rti it may be concluded that RL reflects the degree of bronchoconstriction, in general, different dependences of Rti and Raw on the agonist doses have been observed.

Although it would be difficult to establish the dose equivalence of histamine administered by means of inhalation and infusion, we think that the range of infusion rates used in the present investigation represented, in the context of the studies cited above, challenges varying from small to moderate for the lung as a whole. In about one-half of the cases, the lowest rate of infusion led to no or negligibly small changes in the airway and tissue parameters. Thus we may regard the present results as reflecting relatively sensitive responses of the parenchymal and airway compartments to the constrictor stimuli. The major aspects of a discussion of our findings are *1*) the distribution of airway constriction, as inferred from the Raw, Raw,t and R0 data, and *2*) the relationship between the airway and tissue responses.

Airway responses. The three measures of Raw estimated from our experiments correspond to different underlying structures. Raw is obtained as the Newtonian resistance in the lungs; it has previously been shown (2, 23, 26) that in the normal lungs this component is attributed overwhelmingly to the overall flow resistance in the airways, and there is no indication of a significant Newtonian resistance arising in the constricted parenchyma. By contrast, R0 is a local quantity determined from retrograde impedance measurements through the capsule. It is plausible that on proceeding downstream from the capsule along airway segments of increasing diameter, the resistance accumulates in progressively smaller increments and thus R0 will be

determined profoundly by the most peripheral structures. In agreement with this, the R0 values we observed in the control state were high, although locally variable (from 244 to 8,008 $cmH_2O \cdot s \cdot l^{-1}$); lower values (from 100 to 400 $cmH_2O \cdot s \cdot l^{-1}$) were obtained in constant flow measurements through large capsules embracing numerous punctures by Sasaki et al. (29). By contrast, from the baseline Zaw,ter data reported by Davey and Bates (8), higher R0 values (from 4,000 to 66,000 $cmH_2O \cdot s \cdot l^{-1}$) are estimated than those in the present study. We recall that, although Zaw,ter corresponds to an almost purely resistive pathway in the control state, a characteristic dependence on frequency develops during histamine infusion (Fig. 3). The latter pattern clearly indicates that in the array of the resistive conduits compliant shunt elements are interposed. Indeed, the Zaw,ter data were well fitted by the three-element model (R_1-C-R_2), although meaningful parameter values could be derived from the characteristically frequency-dependent Zaw,ter data only (see APPENDIX). The fact that a pronounced frequency dependence of Zaw,ter was obtained by Davey and Bates (8) in all control measurements was probably due to the different techniques of establishing the transpleural communication: they ablated the pleura in the 1-mm-diam surface in the capsule, whereas we made two punctures 1 mm deep with a needle. The latter method might have resulted in bigger channels opening into a higher number of peripheral airspaces and leading to lower resistances less influenced by the elastic shunt. It is not clear whether C corresponds to tissue distensibility (8) or alveolar gas compressibility or both; however, it must be located close to the pleural puncture because most of the real part of Zaw,ter is shunted out at high frequencies (Fig. 3). For the aims of the present study, it was nevertheless appropriate to characterize the peripheral airway mechanics by the low-frequency R0 values.

The structural background and the interpretation are the most complex in the case of Raw,t. This quantity has been chosen to represent the overall Raw in several studies (3, 16, 17, 20, 21, 25, 27, 28), although PA has been shown to exhibit remarkable inhomogeneity in the normal lung (2, 4, 11, 12, 15, 22, 26, 32) and especially in the constricted state (11, 15, 22). It is important to realize that the agreement between Raw,t and the global Raw depends critically on the relationship between the measured PA and the mean alveolar pressure. Using a distributed-periphery lung model, we have elucidated the mechanisms beyond the regional variability of Raw,t (15): if PA is measured at the end of a medium-resistance pathway, then it corresponds to some typical or medium value of the distribution of alveolar pressures and the calculated Raw,t will be close to the overall Raw, whereas the higher and lower resistance pathways leading to the alveolar capsule will result in overestimation and underestimation, respectively, of Raw. We note that in the real airway tree the deviations from the average pathway resistance may occur at any airway generation and not necessarily at the very periphery. Thus the changes in R0 and Raw,t need not run in parallel. What these two parameters have in common is that both are obtained from a limited number of capsules affixed to easily accessible surfaces of the lungs, and it is therefore highly incidental whether the Raw,t and R0 values correspond to typical pathways and terminal regions, respectively. With this uncertainty kept in mind, our data for the whole population (Table 1) and the individual dogs (Fig. 6) suggest that the greatest and earliest changes in the bronchoconstrictor tone occur in the lung periphery, and these changes may remain for a long time undetected in the overall Raw values. The peripheral dominance of bronchoconstriction is further supported by the fact that the changes in the purely peripheral R0 exceed those in Raw,t, the latter being influenced by the changes in the proximal airway generations.

Airway vs. tissue responses. Mitzner et al. (24) presented evidence of the mechanical linking between pulmonary elasticity and bronchoconstriction in sheep. By perfusing the bronchial vessels with methacholine, they found that the increase in Raw was associated with a fall in dynamic compliance, whereas a similar concentration of methacholine introduced into the pulmonary circulation did not affect the pulmonary mechanics. They also argued that the contracted conducting airways might similarly lead to an increase in Rti. Subsequent work done in open-chest dogs (3, 17) lent only partial support to the hypothesis connecting the constriction of the bronchial tree and the decrease in lung compliance. To clarify the discrepancies in these studies (3, 17), Bates et al. (1) injected histamine intravenously into dogs at fixed lung volume and monitored the elastic recoil pressure, the dynamic elastance, and the estimates of tissue and airway resistances. From the temporal changes in these parameters, they concluded that most of the change in dynamic tissue elastance and resistance was due to ventilation inhomogeneity caused by nonuniform constriction of the conducting airways. However, they also found that both the elastic recoil pressure and η derived from the dynamic tissue data elevated rapidly to plateaus after the bolus injection of histamine, whereas the estimate of Raw increased in a retarded and steady manner.

Our results are at variance with the hypothesis by Mitzner et al. (24). Increases in G by at least 50% (*dogs 1* and *2*) and as large as 100% of the control level (*dog 4*) occurred without a noticeable change in the Raw values or, within a somewhat narrower range of G/G_{Cont}, in the Raw,t values (Fig. 6). Because the corresponding changes in H were milder but still significant (from 13 to 49%), we can state with confidence that the tissue and airway contractions were dissociated in our experiments. (In view of the excellent agreements between G and Gt and between H and Ht, which we found in the measurements with $R0 < 1.1R0_{Cont}$, it is highly improbable that the elevations in G and H resulted from a bias in the input impedance fitting.) Indeed, if the increase in tissue impedance were due to the airway tree becoming stiffer, as Mitzner et al. (24) suggested, it should have been manifested in an overall decrease in airway caliber. The mechanism proposed by Bates et al. (1) invokes virtual increases in G and H, caused by inhomogeneous airway constriction, the

signs of which are not evident either during most of the increase in G/G_{Cont} in three of the animals we studied (*dogs 3, 4,* and *6*). Whereas this mechanism may be effective at higher levels of constriction, such as those elicited by a bolus injection of histamine (1) and those at the highest infusion rates in the present study, the purely tissue response to the low-rate infusion might be the same phenomenon as reflected by the initial changes in elastic recoil and η (1). Of course, we cannot exclude the possibility of the bias of undersampling, i.e., selecting from the population of late-responding regional lung units in these dogs. However, with all dogs considered, we argue that a high degree of inhomogeneity, needed to produce appreciable virtual increases in G and H, should have been accompanied by an elevation in the overall Raw, although it is theoretically not impossible that contracted regions in parallel with adjacent airways extended (25) could result in an unchanged Raw.

Tissue responses. As demonstrated above (Table 1 and Fig. 4), the histamine-induced elevations in G were always higher than those in H. This fairly uniform finding has been explained either on the basis of changes in the intrinsic tissue properties (10) or by attributing the excess increase in G to interregional flows enhanced by the peripheral inhomogeneity (15, 23). Whatever the mechanism, the changes in G/G_{Cont} can be decomposed formally into two components (20)

$$G/G_{cont} = (\eta/\eta_{cont})\ (H/H_{cont})$$

In contrast to the case of altered lung volume, where the changes in G remain proportional to those in H (14, 23, 28), i.e., η is fairly constant, the parenchymal responses to constrictor agonists include elevations in both H and η (1, 15–18, 23, 25, 27, 28, 30). Our data are fully consistent with the latter fact (Table 1). Interestingly, there is an indication that the relationship between G and H is altered simultaneously with, or probably before the changes in H. The G/G_{Cont} vs. H/H_{Cont} data follow a trajectory different from the η = constant line at the initial, small, and even negative changes (Fig. 4); this suggests that the intrinsic coupling between G and H may impose a lower threshold against the constrictor stimulus than G or H themselves do. This hypothetical dissociation of the H/H_{Cont} and η/η_{Cont} components of G/G_{Cont} is supported by observations in challenged parenchymal strips (10) where the increase in Rti was shown to result from two components with different patterns: a rapid elevation in η and an elongated increase in H. In the whole lungs we studied, an obvious contribution was also made to the disproportionately higher increase in G/G_{Cont} by the pendelluft arising from the enhanced inhomogeneity (1, 2, 15), but this was very unlikely to occur at the small initial changes in G and H where even the most sensitive R0 did not substantiate the airway constriction (Fig. 4).

In summary, we have presented direct evidence of the development of constriction in the most peripheral airways, an inhomogeneous process that remains undetected in the overall Raw for a significant range of agonist doses. Our results also indicate that substantial changes in the parenchymal mechanical properties may occur without alterations in the bronchomotor tone.

APPENDIX

The real and imaginary parts of Zaw,ter (*Eq. 2*) can be written as

$$\mathrm{Re(Zaw,ter)} = [R_2 + R_1(1 + \omega^2R_2^2C)]/(1 + \omega^2R_2^2C)$$

and

$$\mathrm{Im(Zaw,ter)} = -j\omega R_2^2C/(1 + \omega^2R_2^2C)$$

These functions describe a negative-frequency-dependent real part with an inflexion point coinciding with the minimum of the imaginary part, such as those shown in Fig. 3, *bottom*.

If we assume that $\omega^2R_2^2C \ll 1$, the above expressions simplify to

$$\mathrm{Re(Zaw,ter)} \approx R_1 + R_2$$

$$\mathrm{Im(Zaw,ter)} \approx -j\omega R_2^2C$$

which are valid either for the high R_2 impedances at the lowest frequency range (e.g., Fig. 3, *bottom*) or for low R_2 impedances over the whole frequency interval (e.g., Fig. 3, *top*). In this case, from the constant real part and the linearly decreasing imaginary part, it is not possible to estimate R_1, R_2, and C separately.

The authors thank I. Kopasz and L. Vígh for excellent technical assistance.

This study was supported by National Institutes of Health Fogarty International Research Collaboration Award R03-TW-00092 and Hungarian National Research Fund Grant OTKA 2675.

Address for reprint requests: Z. Hantos, Dept. of Medical Informatics, Albert Szent-Györgyi Medical Univ., H-6701 Szeged, PO Box 2009, Hungary (E-mail: hantos@dmi.szote.u-szeged.hu).

Received 22 August 1994; accepted in final form 13 June 1995.

REFERENCES

1. **Bates, J. H. T., A.-M. Lauzon, G. S. Dechman, G. N. Maksym, and T. F. Schuessler.** Temporal dynamics of pulmonary response to intravenous histamine in dogs: effects of dose and lung volume. *J. Appl. Physiol.* 76: 616–626, 1994.
2. **Bates, J. H. T., M. S. Ludwig, P. D. Sly, K. Brown, J. G. Martin, and J. J. Fredberg.** Interrupter resistance elucidated by alveolar pressure measurement in open-chest normal dogs. *J. Appl. Physiol.* 65: 408–414, 1988.
3. **Bates, J. H. T., and R. Peslin.** Acute pulmonary response to intravenous histamine at fixed lung volume in dogs. *J. Appl. Physiol.* 75: 405–411, 1993.
4. **Brusasco, V., D. O. Warner, K. C. Beck, J. R. Rodarte, and K. Rehder.** Partitioning of pulmonary resistance in dogs: effects of tidal volume and frequency. *J. Appl. Physiol.* 66: 1190–1196, 1989.
5. **Csendes, T.** Nonlinear parameter estimation by global optimization—efficiency and reliability. *Acta Cybern.* 8: 361–370, 1988.
6. **Daróczy, B., A. Fabula, and Z. Hantos.** Use of noninteger-multiple pseudorandom excitation to minimize nonlinear effects on impedance estimation. *Eur. Respir. Rev.* 1: 183–187, 1991.
7. **Daróczy, B., and Z. Hantos.** Generation of optimum pseudorandom signals for respiratory impedance measurements. *Int. J. Biomed. Comput.* 25: 21–31, 1990.
8. **Davey, B. L. K., and J. H. T. Bates.** Regional lung impedance from forced oscillations through alveolar capsules. *Respir. Physiol.* 91: 165–182, 1993.
9. **Franken, H., J. Clément, M. Cauberghs, and K. P. Van de Woestijne.** Oscillating flow of a viscous compressible fluid

through a rigid tube: a theoretical model. *IEEE Trans. Biomed. Eng.* 28: 416–420, 1981.
10. **Fredberg, J. J., D. Bunk, E. Ingenito, and S. A. Shore.** Tissue resistance and the contractile state of lung parenchyma. *J. Appl. Physiol.* 74: 1387–1397, 1993.
11. **Fredberg, J. J., R. H. Ingram, Jr., R. G. Castile, G. M. Glass, and J. M. Drazen.** Nonhomogeneity of lung response to inhaled histamine assessed with alveolar capsules. *J. Appl. Physiol.* 58: 1914–1922, 1985.
12. **Fredberg, J. J., D. H. Keefe, G. M. Glass, R. G. Castile, and I. D. Frantz III.** Alveolar pressure nonhomogeneity during small-amplitude high-frequency oscillation. *J. Appl. Physiol.* 57: 788–800, 1984.
13. **Fredberg, J. J., and D. Stamenović.** On the imperfect elasticity of lung tissue. *J. Appl. Physiol.* 67: 2408–2419, 1989.
14. **Hantos, Z., B. Daróczy, T. Csendes, B. Suki, and S. Nagy.** Modeling of low-frequency pulmonary impedance in dogs. *J. Appl. Physiol.* 68: 849–860, 1990.
15. **Hantos, Z., B. Daróczy, B. Suki, S. Nagy, and J. J. Fredberg.** Input impedance and peripheral inhomogeneity of dog lungs. *J. Appl. Physiol.* 72: 168–178, 1992.
16. **Ingenito, E. P., B. Davison, and J. J. Fredberg.** Tissue resistance in the guinea pig at baseline and during methacholine constriction. *J. Appl. Physiol.* 75: 2541–2548, 1993.
17. **Lauzon, A.-M., G. Dechman, and J. H. T. Bates.** Time course of respiratory mechanics during histamine challenge in the dog. *J. Appl. Physiol.* 73: 2643–2647, 1992.
18. **Loring, S. H., J. M. Drazen, J. C. Smith, and F. G. Hoppin, Jr.** Vagal stimulation and aerosol histamine increase hysteresis of lung recoil. *J. Appl. Physiol.* 51: 477–484, 1981.
19. **Ludwig, M. S., I. Dreshaj, J. Solway, A. Munoz, and R. H. Ingram, Jr.** Partitioning of pulmonary resistance during constriction in the dog: effects of volume history. *J. Appl. Physiol.* 62: 807–815, 1987.
20. **Ludwig, M. S., F. M. Robatto, S. Simard, J. Sato, D. Stamenović, and J. J. Fredberg.** Lung tissue resistance during contractile stimulation: the structural damping decomposition. *J. Appl. Physiol.* 72: 1332–1337, 1992.
21. **Ludwig, M. S., F. M. Robatto, P. D. Sly, M. Browman, J. H. T. Bates, and P. V. Romero.** Histamine-induced constriction of canine peripheral lung: an airway or tissue response? *J. Appl. Physiol.* 71: 287–293, 1991.
22. **Ludwig, M. S., P. V. Romero, and J. H. T. Bates.** A comparison of the dose-response behavior of canine airways and parenchyma. *J. Appl. Physiol.* 67: 1220–1225, 1989.
23. **Lutchen, K. R., B. Suki, Q. Zhang, F. Peták, B. Daróczy, and Z. Hantos.** Airway and tissue mechanics during physiological breathing and bronchoconstriction in dogs. *J. Appl. Physiol.* 77: 373–385, 1994.
24. **Mitzner, W., S. Blosser, D. Yager, and E. Wagner.** Effect of bronchial smooth muscle contraction on lung compliance. *J. Appl. Physiol.* 72: 158–167, 1992.
25. **Nagase, T., A. Moretto, and M. S. Ludwig.** Airway and tissue behavior during induced constriction in rats: intravenous vs. aerosol administration. *J. Appl. Physiol.* 76: 830–838, 1994.
26. **Peták, F., Z. Hantos, Á. Adamicza, and B. Daróczy.** Partitioning of pulmonary impedance: modeling vs. alveolar capsule approach. *J. Appl. Physiol.* 75: 513–521, 1993.
27. **Romero, P. V., and M. S. Ludwig.** Maximal methacholine-induced constriction in rabbit lung: interactions between airways and tissue. *J. Appl. Physiol.* 70: 1044–1050, 1991.
28. **Romero, P. V., F. M. Robatto, S. Simard, and M. S. Ludwig.** Lung tissue behavior during methacholine challenge in rabbits in vivo. *J. Appl. Physiol.* 73: 207–212, 1992.
29. **Sasaki, H., T. Takishima, and M. Nakamura.** Collateral resistance at alveolar level in excised dog lungs. *J. Appl. Physiol.* 48: 982–990, 1980.
30. **Sly, P. D., and C. J. Lanteri.** Differential responses of the airways and pulmonary tissues to inhaled histamine in young dogs. *J. Appl. Physiol.* 68: 1562–1567, 1990.
31. **Van de Woestijne, K. P., H. Franken, M. Cauberghs, F. J. Lándsér, and J. Clément.** A modification of the forced oscillation technique. In: *Advances in Physiological Sciences. Respiration. Proceedings of the 28th International Congress of Physiological Sciences*, edited by I. Hutás and L. A. Debreczeni. Oxford, UK: Pergamon, 1981, vol. 10, p. 655–660.
32. **Warner, D. O.** Alveolar pressure inhomogeneity during low-frequency oscillation of excised canine lobes. *J. Appl. Physiol.* 69: 155–161, 1990.

II

Methacholine-induced bronchoconstriction in rats: effects of intravenous vs. aerosol delivery

FERENC PETÁK, ZOLTÁN HANTOS, ÁGNES ADAMICZA,
TIBOR ASZTALOS, AND PETER D. SLY
Institute for Child Health Research, Perth, Western Australia 6001, Australia; and Department of Medical Informatics and Engineering and Institute of Experimental Surgery, Albert Szent-Györgyi Medical University, H-6701 Szeged, Hungary

Peták, Ferenc, Zoltán Hantos, Ágnes Adamicza, Tibor Asztalos, and Peter D. Sly. Methacholine-induced bronchoconstriction in rats: effects of intravenous vs. aerosol delivery. *J. Appl. Physiol.* 82(5): 1479–1487, 1997.—To determine the predominant site of action of methacholine (MCh) on lung mechanics, two groups of open-chest Sprague-Dawley rats were studied. Five rats were measured during intravenous infusion of MCh (iv group), with doubling of concentrations from 1 to 16 $\mu g \cdot kg^{-1} \cdot min^{-1}$. Seven rats were measured after aerosol administration of MCh with doses doubled from 1 to 16 mg/ml (ae group). Pulmonary input impedance (Z_L) between 0.5 and 21 Hz was determined by using a wave-tube technique. A model containing airway resistance (Raw) and inertance (Iaw) and parenchymal damping (G) and elastance (H) was fitted to the Z_L spectra. In the iv group, MCh induced dose-dependent increases in Raw [peak response 270 ± 9 (SE) % of the control level; $P < 0.05$] and in G (340 ± 150%; $P < 0.05$), with no increase in Iaw (30 ± 59%) or H (111 ± 9%). In the ae group, the dose-dependent increases in Raw (191 ± 14%; $P < 0.05$) and G (385 ± 35%; $P < 0.05$) were associated with a significant increase in H (202 ± 8%; $P < 0.05$). Measurements with different resident gases [air vs. neon-oxygen mixture, as suggested (K. R. Lutchen, Z. Hantos, F. Peták, Á. Adamicza, and B. Suki. *J. Appl. Physiol.* 80: 1841–1849, 1996)] in the control and constricted states in another group of rats suggested that the entire increase seen in G during the iv challenge was due to ventilation inhomogeneity, whereas the ae challenge might also have involved real tissue contractions via selective stimulation of the muscarinic receptors.

airway resistance; lung tissue resistance; forced oscillations

PREVIOUS STUDIES on respiratory mechanics at frequencies above those of spontaneous breathing rate or performed on isolated airways led to the belief that methacholine (MCh) causes constriction merely of the conducting airways. Recently, partitioning of the lung resistance (R_L) into airway (Raw) and parenchymal (Rti) parts has established the importance of the lung tissues in the pulmonary responsiveness to various constrictor stimuli (11, 13, 14, 18, 19, 21–27). Nevertheless, numerous conflicting data have been reported on the site of action of bronchoactive agonists such as MCh or histamine. In a number of studies, the pulmonary tissue has been shown to be responsible for the major increase in the resistive pressure drop across the lungs after a MCh aerosol challenge (18, 27) or after a bolus intravenous (iv) infusion (13). Inhalation of MCh was reported to elevate Raw and Rti to a similar degree in dogs (21). In contrast, no increase was observed in the parenchymal hysteresis in humans after a MCh aerosol challenge, whereas the airways seemed to respond (14, 19). In all of the above studies the airways were demonstrated to respond to a MCh challenge, but practically no increase in Raw was detected in rabbits after MCh inhalation, whereas the Rti and elastance increased eight- and threefold, respectively (22). Furthermore, Sato et al. (24) found a fairly uniform tissue constriction, whereas Raw displayed an obvious elevation in two dogs, only a slight increase in a third, and even a decrease in the fourth.

Recently, Nagase et al. (18) investigated the mechanism that gives rise to Rti, by inducing constriction with an iv or aerosol administration of MCh. They demonstrated that aerosolized MCh had a greater effect on the airways, whereas iv delivery generated higher parenchymal responses. They argued that the latter phenomenon may be related to a heterogeneous response of the peripheral airways. More recently, by provoking smaller increases in Rti, Salerno et al. (23) obtained a fundamentally different pattern of effect, depending on whether the MCh was inhaled or iv delivered.

Most of these contradictions can be attributed to methodological factors. Both in vivo and in vitro studies have suggested that MCh increases the inhomogeneity of the lung periphery (11, 18), and it has been pointed out that, in the presence of a peripheral inhomogeneity, the uncertainties associated with the sampling of alveolar pressure (P_A) with alveolar capsules may lead to false estimations of airway and tissue responses to constrictor stimuli (11). It should be also recalled that the vast majority of the studies referred to above used alveolar capsules to sample P_A. On the other hand, it has been demonstrated that model parameters derived from low-frequency pulmonary input impedance data (Z_L) adequately characterize the airway and lung tissue properties both under control conditions (8–12, 15, 16, 20, 24, 28) and during pulmonary constriction (11, 12, 15, 17).

It is unclear what portion of the contradictory data relating to the relative contributions of the airways and parenchyma to MCh-induced constriction can be attributed to the different routes of MCh delivery. The purpose of the present study was a systematic exploration of how the predominant site of action of MCh in the respiratory tract differs, depending on the route of administration, within a single strain of rat. To avoid any possible carryover effect, the studies were performed in two separate groups of rats. In the first group of rats, MCh was infused iv, whereas the second group was challenged with aerosolized MCh. Overall airway

and lung tissue responses were separated by fitting a model containing an airway and a parenchymal compartment to low-frequency Z_L data (11).

METHODS

Animal Preparation

We performed experiments in two groups of adult male Sprague-Dawley rats. MCh was administered iv to five rats (330–450 g; iv group), and eight rats [340–410 g; aerosol (ae) group] were used to examine the effect of inhaled MCh. In both groups, the animals were anesthetized with pentobarbital sodium (30 mg/kg ip) and placed in a supine position on a heating pad. A carotid artery and a jugular vein were cannulated for monitoring of systemic blood pressure and drug delivery, respectively. Tracheostomy was performed, and a 30-mm plastic cannula (2-mm inner diameter) was inserted into the distal trachea. Mechanical ventilation was maintained by a Harvard small-animal respirator, with a tidal volume of 3 ml and a frequency of 90 breaths/min. The end-expiratory pressure was set at 2.5 cmH_2O, the thorax was opened with midline sternotomy, and the ribs were widely retracted. Paralysis was accomplished with pipecuronium bromide (0.2 mg/kg initial dose, supplemented every 20 min by 0.05 mg/kg). Additional anesthetics (10 mg/kg pentobarbital sodium) were given every 40 min.

Z_L Measurements

Z_L was measured with the wave-tube technique (6, 12, 29). The tracheal cannula was switched from the respirator at end expiration and connected to a loudspeaker-in-box system through a 120-cm length of polyethylene tubing (2-mm inner diameter). Before each measurement, the pressure in the box chambers was adjusted to 2.5 cmH_2O to keep the transpulmonary pressure unchanged during measurements. The wave-tube was equipped with sidearms and miniature transducers (ICS model 33NA002D) to measure the lateral pressures at the loudspeaker end (P_1) and the cannula end (P_2). The loudspeaker was driven by a computer-generated small-amplitude pseudorandom signal containing 23 noninteger-multiple components between 0.5 and 21 Hz and producing a <2-cmH_2O peak-to-peak excursion in P_1. The signals of P_1 and P_2 were low-pass filtered (5th-order Butterworth, 25-Hz corner frequency) and digitized at a sampling rate of 128 Hz by an analog-to-digital board of an AT486 IBM-compatible computer. The pressure-transfer functions (i.e., P_1/P_2) were computed by fast Fourier transformation from the 6-s recordings by using 4-s time windows and 95% overlapping. According to the transmission line theory, Z_L can be calculated from the P_1/P_2 spectra as the load impedance of the wave tube (6, 12, 29)

$$Z_L = Zo \sinh(\gamma L)/[(P_1/P_2) - \cosh(\gamma L)]$$

where Zo and γ are the characteristic impedance and the complex propagation wave number, respectively, both determined by the geometrical data and the material constants of the tube and the air (4).

Study Protocol

iv Challenge. MCh was infused at rates of 1, 2, 4, 8, or 16 $\mu g \cdot kg^{-1} \cdot min^{-1}$. Before each infusion, the lungs were hyperinflated by occluding the expiratory outlet of the respirator for one cycle, i.e., producing two superimposed inspirations. Four successive measurements of Z_L, 1 min apart, were made and the infusion was then started. The duration of each infusion was 10 min, and Z_L was measured 30 s after the onset of the infusion and every 1 min thereafter. The infusion was suspended for at least 15 min to let the blood pressure recover before the next series of control and infusion measurements was begun.

Aerosol challenge. After four successive baseline measurements, solutions of saline or 1, 2, 4, 8, or 16 mg/kg MCh were delivered for 40 s each by an ultrasonic nebulizer (model 2000, DeVilbiss) via the inspiratory port of the respirator. Before each delivery, two inspiratory phases were superimposed to standardize the volume history. Measurements were started 30 s after completion of each aerosol challenge, and six successive recordings were collected during every 30 s. The next dose was administered 60 s after the last recording.

Parameter Estimation

The Z_L data were evaluated in terms of a model containing an airway compartment characterized by frequency-independent resistance (Raw) and inertance (Iaw) and a constant-phase tissue compartment including tissue damping (G) and elastance (H)

$$Z_L = Raw + j\omega Iaw + (G - jH)/\omega^{\alpha}$$

where j is the imaginary unit, ω is the angular frequency, and exponent α is expressed as $\alpha = 2/\pi \arctan(H/G)$. Pulmonary hysteresivity (η) (7) was calculated as G/H.

In the iv group, three to five Z_L spectra were ensemble averaged in each preinfusion state and at the peak responses. Because of the absence of a plateau response after the MCh aerosol challenge, parameters corresponding to the peak response in Raw were used for analysis in the ae group. The data at frequencies coinciding with the heart rate and its harmonics were often corrupted, as evidenced by poor coherence and a high SD, and they were omitted from the model fitting.

Statistical Analysis

Scatters in the parameters were expressed in SE values. We used one-way analysis of variances with Dunnett's multiple comparison procedure to compare the parameters from the control with those obtained after MCh challenges. Two-way analysis of variances with the Student-Newman-Keuls multiple comparison procedure was applied to compare the effects of iv and aerosolized MCh. Each test was performed with a $P < 0.05$ significance level.

Validation of Airway-Tissue Separation

To validate the airway and tissue parameters derived from model fitting, we measured another group of animals breathing air and then a mixture of 80% neon + 20% oxygen (NeOx) under both control and steady-state constricted conditions, as suggested by Lutchen et al. (15). Three rats were challenged with 16 and 32 $\mu g \cdot kg^{-1} \cdot min^{-1}$ iv infusions of MCh, and three were challenged with 4 mg/ml aerosolized MCh. To allow for measurements both with air and with NeOx, a stable level of constriction was required. This was achieved by continuing each challenge for 30 min.

We used a modified setup to collect Z_L data. The wave tube was not directly connected to the loudspeaker box. To allow for accurate control of the gas concentration in the system as well as rapid change in the composition of the oscillatory gas, a bag-in-box system was inserted between the loudspeaker and the wave tube. The loudspeaker oscillated the air in the box, and the opening of the bag was led transmurally to the wave tube. The material constants of the air or the NeOx were used to calculate Zo and γ.

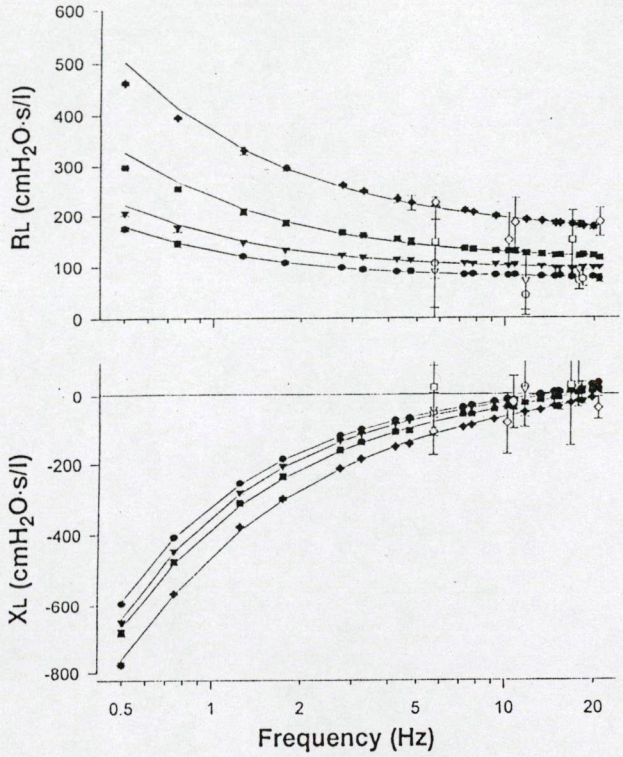

Fig. 1. Real [i.e., lung resistance (R_L)] and imaginary [i.e., lung reactance (X_L)] parts of pulmonary impedance in a representative rat under control conditions (●) and during 2 (▼), 4 (■), or 8 (◆) $\mu g \cdot kg^{-1} \cdot min^{-1}$ intravenous methacholine (MCh) infusions, respectively. Values are means ± SD; n = average of 3–5 successive measurements under each condition. Lines, corresponding model fits. Impedance data corrupted by cardiac noise were omitted from model fit (open symbols).

Before the NeOx measurements, four to six data epochs each were collected when the lungs were filled with room air at baseline and when a steady-state constriction was observed. The rats were then switched to breathe NeOx from a reservoir attached to the inspiratory port of the respirator. When the NeOx concentration had equilibrated (~90 breaths), four to six measurements were made with the NeOx-filled bag in the box.

RESULTS

Typical Z_L data recorded in the control state and at three iv MCh-infusion rates are presented in Fig. 1. The low variabilities of the Z_L data indicate very stable plateau responses in this animal. MCh caused increases in the real part of Z_L (i.e., R_L) at all frequencies, but they were more obvious in the low-frequency range; in general, these elevations were accompanied by minor changes in pulmonary reactance (X_L) in the iv group but by more marked decreases in X_L in the ae group. Apart from the small systematic fitting error in the two lowest-frequency points of the real parts during MCh challenge, the model fits the Z_L data well, with an average fitting error (F) of 2.6 ± 0.1% in the ae group and 2.9 ± 0.1% in the iv group, respectively. F showed no statistically significant differences between the control and the constricted states in either group. There were no statistically significant differences between the baseline parameter values from the two groups.

iv Challenge

Figure 2 summarizes the airway and tissue parameters obtained in the control state and at the different MCh-infusion rates. Similar MCh-induced elevations occurred in Raw, G, and η, which reached 270 ± 90% ($P < 0.05$), 340 ± 150% ($P < 0.05$), and 301 ± 102% ($P < 0.05$), respectively, of their control values. We observed no significant changes in Iaw or in H throughout the infusions, although Iaw in one rat displayed a marked decrease during the highest infusion rate, causing a fall in the average value. No residual effect of iv MCh was found; every parameter returned to its baseline value between infusions (data not presented).

Aerosol Challenge

Changes in the averaged airway and parenchymal parameters for the ae group are shown in Fig. 3 for control and MCh challenges. None of the model parameters exhibited significant changes after saline nebulization. Inhalation of increasing concentrations of MCh caused monotonous and statistically significant elevations in all parameters except Iaw, with the changes beginning after the 2 mg/kg concentration. In response to the highest dose, Iaw was seen to decrease significantly. The group mean values of Raw, Iaw, G, and η at peak response were 191 ± 14 ($P < 0.05$), 73 ± 8 ($P < 0.05$), 385 ± 35 ($P < 0.05$), and 190 ± 13% ($P < 0.05$), respectively, of the control levels. In contrast to the iv MCh challenge, monotonic and statistically significant elevations were found in H, which increased after the highest dose to 202 ± 8% ($P < 0.05$) of the control value.

Airway and Tissue Responses: Aerosol vs. iv Delivery

To examine further the differences in the predominant site of action of MCh on lung mechanics, depending on the route of delivery, in Fig. 4 we have plotted the model parameters for the iv group against the corresponding values for the ae group, both normalized by the control values. If the pattern of change were the same in response to iv and aerosol challenges, we would expect a linear relationship between the changes in each variable, with the dose equivalence between the two routes of delivery represented by the slope of the relationship. Different slopes for different variables would indicate a difference in the relative dose-response characteristics for the two delivery routes. In fact, our data demonstrate quite different relationships for different variables. A two-way analysis of variance, with the route of challenge as the first and the dose of MCh as the second factor, revealed that iv administration of MCh induced a significantly higher Raw and a lower Iaw than those after the aerosol challenge. The increases in G were significantly higher in response to the inhalation challenge than after the iv challenge of successive doses. The relative changes in H were highly dissociated: statistically significantly greater elevations were found for the last three aerosol doses than for the corresponding iv concentrations. As follows from the different patterns in G and H, the iv MCh increased

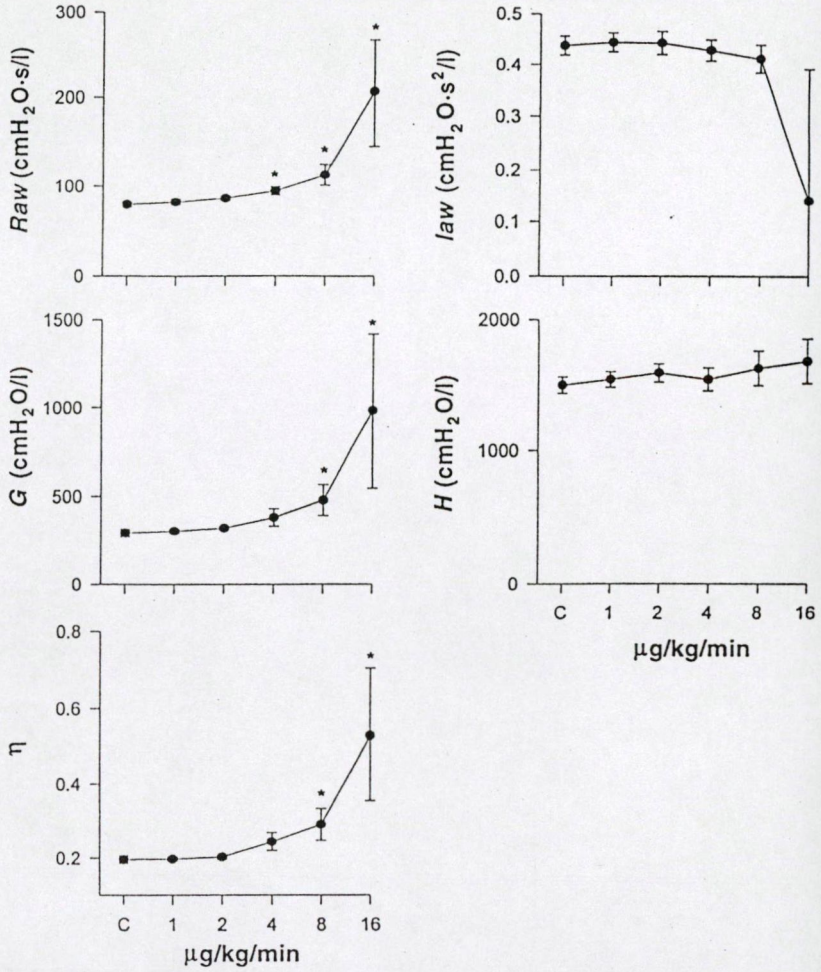

Fig. 2. MCh dose-response curves for airway resistance (Raw), airway inertance (Iaw), tissue damping (G) and tissue elastance (H), and pulmonary hysteresivity (η) in iv group. C, control. *Significantly different from control, $P < 0.05$.

η significantly more than did the corresponding aerosol dose.

The statistical analysis also revealed that, irrespective of the route factor (i.e., ae or iv), MCh exerted highly significant effects on all parameters ($P < 0.005$). Furthermore, independently of the dose factor, the changes in Raw, Iaw, and η were not different in the two populations, whereas the relative changes in G and H in the ae group were significantly greater than those in the iv group ($P < 0.02$ and $P < 0.001$, respectively).

Model Validation

In both groups of rats involved in the NeOx experiments, when the lungs were filled with air, MCh induced a pattern of change in the model parameters similar to that obtained in the main groups of animals (Figs. 2 and 3), although the exposure of the animals to aerosolized MCh was different from that for the main group of rats (continuous aerosol challenge). For the animals breathing air, Raw increased (63 ± 11%) and Iaw slightly decreased (−11 ± 4%) after the 16 $\mu g \cdot kg^{-1} \cdot min^{-1}$ MCh infusion. An increase in G (35 ± 18%) was seen, with practically no change in H (14 ± 10%). In the rats challenged with 4 mg/ml aerosolized MCh, a moderate increase in Raw (24 ± 18%) and no change in Iaw (9 ± 7%) occurred. The increase in G (125 ± 97%) was accompanied by an increase in H (86 ± 58%).

To evaluate the differences due to the change of the resident gas in the lungs, we calculated the NeOx-to-air parameter ratios. When a steady-state NeOx concentration is established in the lungs, the physical principles would lead to the expectation that Raw_{NeOx}/Raw_{air} reflects the predicted ratio of the viscosities (1.4), whereas Iaw_{NeOx}/Iaw_{air} reflects that of the densities (0.8) of the two gas mixtures. Furthermore, as Lutchen et al. (15) argued, the tissue parameters should be independent of the resident gas in the normal lung. Figure 5 shows these data for the rats challenged with iv MCh. In the control condition, the ratios for Raw and Iaw were 1.47 ± 0.04 and 0.75 ± 0.06, respectively. The estimates of G and H were independent of the resident gas, as shown by ratios not significantly different from unity (1.0 ± 0.0 and 0.96 ± 0.05 for G and H, respectively). During 16 $\mu g \cdot kg^{-1} \cdot min^{-1}$ MCh infusion, the ratios of Raw (1.39 ± 0.01) and Iaw (0.76 ± 0.06) were similar to those obtained under control conditions. No systematic dependence on the intrapulmonary gas was found for H (1.04 ± 0.09), whereas the ratio of G increased (1.16 ± 0.06). After elevation of the MCh dose to 32 $\mu g \cdot kg^{-1} \cdot min^{-1}$, the NeOx-to-air ratios of Raw and

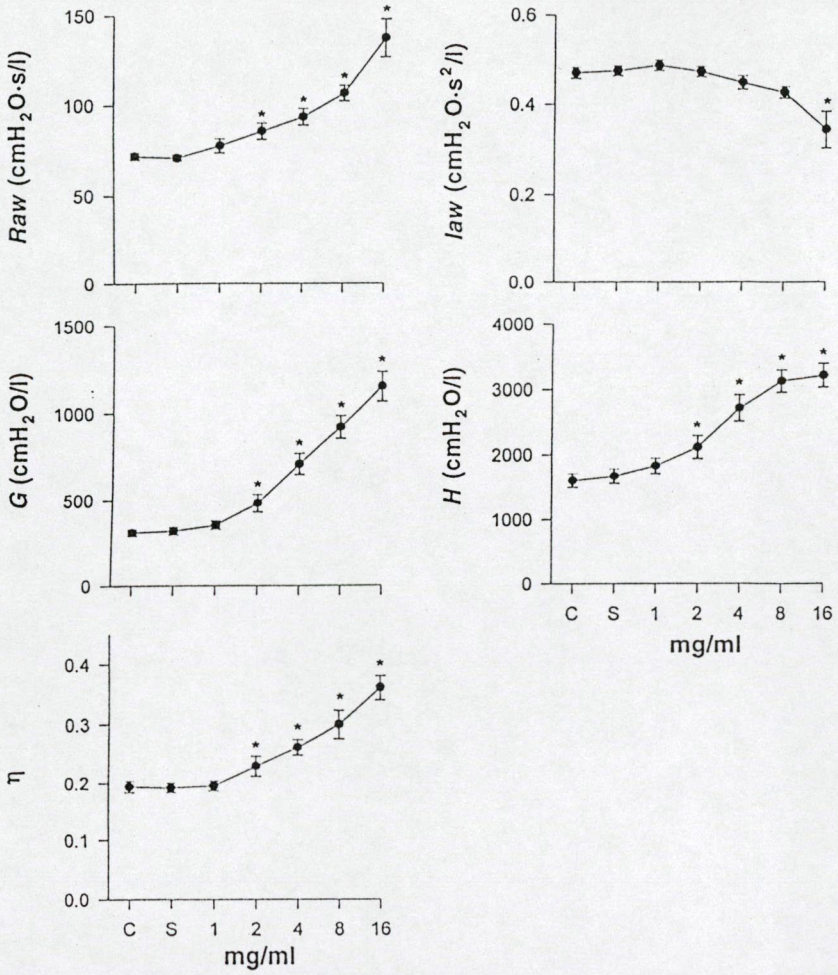

Fig. 3. MCh dose-response curves for Raw, Iaw, G, H, and η in aerosol administration of MCh (ae) group. S, saline. *Significantly different from control, $P < 0.05$.

H remained unchanged (1.46 ± 0.07 and 1.01 ± 0.02, respectively), whereas that of G increased further (1.27 ± 0.15) and Iaw_{NeOx}/Iaw_{air} decreased (0.49 ± 0.08).

The NeOx-to-air parameter ratios for the control conditions and during continuous 4 mg/kg aerosolized MCh challenge are shown in Fig. 6. The ratios obtained under control conditions were very similar to those obtained during MCh infusion. The ratio of Raw again reflects the difference in the gas viscosities (1.47 ± 0.03), whereas the Iaw ratio shows the effect of the different densities (0.72 ± 0.05). The estimates of both G (1.02 ± 0.02) and H (1.03 ± 0.03) were not sensitive to the resident gas in the lungs. Like the moderate iv challenge, the constriction induced by aerosolized MCh had no influence on the ratios of Raw (1.53 ± 0.08), Iaw (0.71 ± 0.03), or H (1.06 ± 0.05). However, G again showed a marked gas dependence (1.21 ± 0.11) during constriction.

DISCUSSION

To examine whether the site of action of MCh differs, depending on the route of administration, we partitioned the response of the lung into airway and parenchymal components when the agent was either inhaled or administered iv. We found significant differences between inhalation and iv delivery. The iv challenge induced roughly a threefold increase in Raw and similar elevation in G. No increases in Iaw or H were seen. The different patterns of change in G and H resulted in marked elevations in η. The aerosol delivery of MCh induced two- and fourfold increases in Raw and G, respectively. In contrast with the iv delivery, a twofold, highly significant elevation was also observed in H. The combination of the patterns in the tissue parameters resulted in a moderate elevation in η.

Model Appropriateness

Our Z_L spectra agree qualitatively with those reported on dogs (10–12, 24, 28), cats (8), and rabbits (16) and are very similar to those obtained in rats (9, 15). The ability of the constant-phase model to afford an accurate description of the tissue mechanics and thereby separate the airway and parenchymal components of the total Z_L has been demonstrated in different species under control (8, 10–12, 15, 16, 20, 28) and constricted conditions (11, 12, 15, 17). Both in the present study and in previous reports, the model fitted equally well to Z_L data obtained after aerosol and iv challenges. Our confidence in the model performance is reinforced by

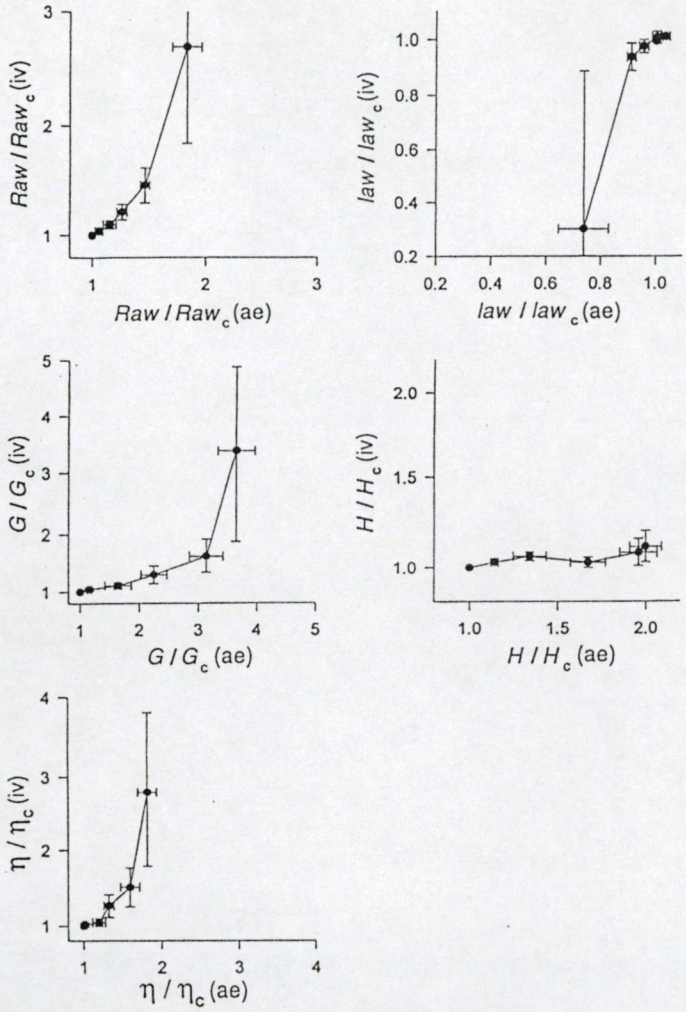

Fig. 4. Comparison of parameter values obtained during ae and iv delivery of MCh, all normalized by their control (c) values. See text for details.

the results of the present model validation studies involving the use of different resident gases. In agreement with the results reported by Lutchen et al. (15), the baseline lung tissue properties were not affected when the intrapulmonary air was replaced by NeOx, and the ratios of Raw and Iaw reflected the viscosity and density ratios, respectively, of the intrapulmonary gases. Accordingly, our data confirm their conclusion, i.e., airway inhomogeneities do not influence the estimates of airway and parenchymal mechanics from low-frequency ZL spectra obtained under control conditions. In addition, during both iv and aerosolized delivery of MCh, the NeOx-to-air ratios of Raw, Iaw, and H remained at the baseline level, whereas G was higher when the lung was filled with NeOx. This finding is also fully consistent with the results of Lutchen et al. (15), confirming that airflow inhomogeneities due to heterogeneous constriction of the peripheral airways can contribute to an increase in G.

Predominant Site of Action of MCh

iv Infusion. Our data indicate that MCh delivered by iv infusion has a significant effect on the airway caliber. Furthermore, our dose-response curves permit an insight into the serial distribution of the bronchoconstriction. MCh induced a significant increase in Raw, whereas Iaw remained at the baseline level at doses producing moderate constriction. Because Iaw is thought to be primarily a property of the central airways, it may be concluded that iv MCh induced bronchoconstriction in the peripheral airways.

The interpretation of the parenchymal response is not as obvious and requires a short review of the assumptions inherent in the partitioning method. We assume that the asymptotic value of the real part represents the frequency-independent Raw, and the entire frequency dependence of the low-frequency real and imaginary parts can be attributed to the viscoelasticity of the parenchyma. At baseline, our tissue parameters were independent of the resident gas in the lungs, confirming that these assumptions are likely to be valid in healthy lungs (15).

The G_{NeOx}/G_{air} ratio increased from 1.00 at baseline to 1.16 and 1.27 during iv MCh infusion at 16 and 32 $\mu g \cdot kg^{-1} \cdot min^{-1}$, respectively. This finding also confirms the observation of Lutchen et al. (15) that the enhanced airway inhomogeneity induced by severe constriction can add a significant artifactual (i.e., not of tissue origin) frequency dependence to the low-frequency real part, and hence G. Consequently, a MCh-induced elevation in G can either occur as a result of changed intrinsic tissue damping or originate from peripheral ventilation inhomogeneity.

After iv administration, we found a significant (4-fold) increase in G, whereas H remained at the baseline level. This finding is similar to the results obtained by Lutchen et al. (15) in Wistar rats, although they observed a slight (12.8%) but statistically significant elevation in H during the 16 $\mu g \cdot kg^{-1} \cdot min^{-1}$ MCh

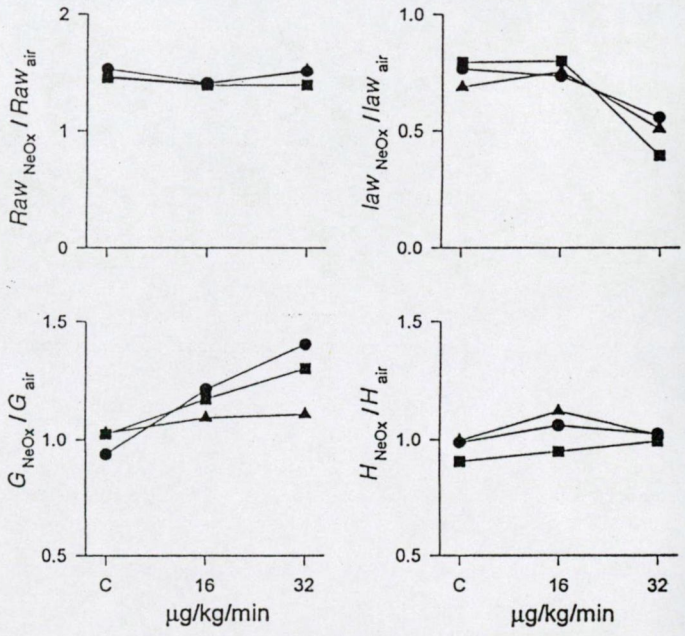

Fig. 5. Ratios of Raw, Iaw, G, and H obtained with a mixture of 80% neon + 20% oxygen (NeOx) relative to room air in control and during 16 or 32 $\mu g \cdot kg^{-1} \cdot min^{-1}$ iv MCh infusions in 3 individual rats.

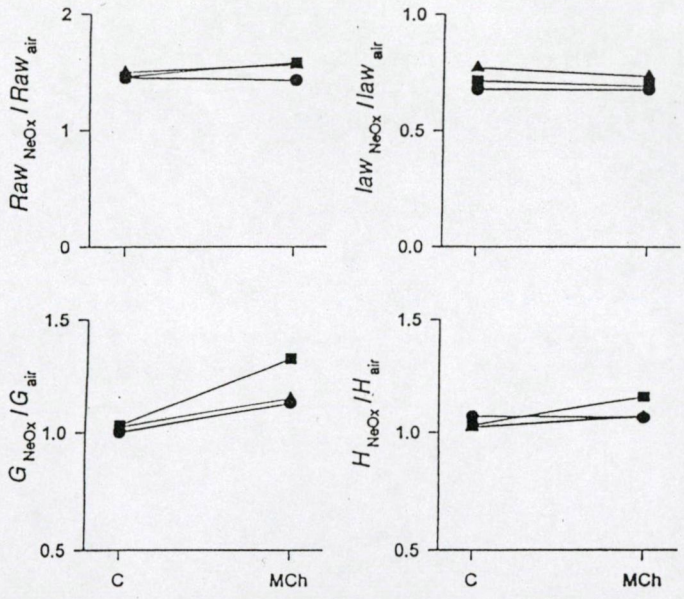

Fig. 6. Ratios of Raw, Iaw, G, and H obtained with NeOx relative to room air in control and after a 4 mg/ml aerosolized MCh challenge in 3 individual rats.

infusion, which accompanied a marked (44%) increase in G. They argued that enhanced airway inhomogeneities increased the frequency dependence of RL and lung elastance (EL).

The MCh-induced changes in the parameters obtained in the present study during iv administration suggest the same phenomenon: the entire increase in G during iv challenge is likely to be artifactual and can be attributed solely to inhomogenous airway constriction. Alternatively, it may be assumed that the lack of change in one of the primary determinants of tissue mechanics (H) was accompanied by increases in η, the other primary tissue parameter (5), and this was reflected by the elevated values of G ($= \eta H$). Although our supplementary measurements with different resident gases (Fig. 5) substantiate that peripheral airway inhomogeneity was the major contributor to the increase in G (and η), we cannot exclude the possible involvement of an altered tissue hysteresivity.

The notion of pure airway constriction in response to an iv MCh challenge is somewhat surprising and contradicts all of the previous studies. In the same rat strain that we used in the present study, Nagase et al. (18) partitioned airway and lung tissue responses to an iv MCh challenge. They used alveolar capsules and multilinear regression analysis of the airway opening pressure, tracheal airflow, and PA signals during mechanical ventilation to calculate lung mechanics and found approximately five- and threefold elevations in Rti and EL, respectively. Similar results were reported in guinea pigs by Ingenito et al. (13), who calculated the enclosed area of the pressure-volume curves seen at the airway opening and in alveolar capsules. However, when the dose of iv-administered MCh was restricted to modest levels, Salerno et al. (23) reported a fundamentally different tissue response in Brown Norway rats. They found that Rti approximately doubled, whereas the highest increase in EL was <20%. Similarly, Sato et al. (24) reported that Rti was doubled after an iv bolus of MCh in dogs, whereas the increase in EL was 30–50%. In addition to methodological differences between those reports and the present study (tidal ventilation vs. small-amplitude oscillation at functional residual capacity), it should also be pointed out that we use a frequency-independent elastance coefficient (H), whereas the EL values reported above were effective elastances calculated at respiratory frequencies. Indeed, the EL values calculated from our XL data at 1.75 Hz (a frequency typically applied in rat studies with alveolar capsules) revealed dose-dependent increases in EL, reaching statistically significant levels during 8 (26 ± 11%, $P < 0.05$) and 16 $\mu g \cdot kg^{-1} \cdot min^{-1}$ (91 ± 58%, $P < 0.05$) MCh infusions. As pointed out by Lutchen et al. (15), this discrepancy between the MCh-induced changes in EL and H can be attributed to the phenomenon that peripheral airway inhomogeneities leading to increases in G may also increase the positive frequency dependence of the effective EL, whereas the intrinsic elastic and resistive properties of the tissues do not change.

Aerosol challenge. The aerosol administration of MCh results in a similar pattern of change in the airway parameters to that observed during iv challenge. Therefore, the above considerations allow the conclusion that constriction occurred in the peripheral airways. We additionally found consistent and significant increases in both G and H, although those in G were always higher than those in H. Accordingly, consistent and significant elevations were found in η. The elevations in G can either be explained on the basis of changes in intrinsic tissue properties (5) or, to some extent, can be attributed to increased peripheral inhomogeneities (3, 11, 15, 17). The results of our NeOx experiments during an aerosolized MCh challenge indeed confirm that the estimation of G is influenced by inhomogeneities. Nevertheless, the dose-dependent elevations in H suggest that aerosolized MCh induced constriction in both the airways and the parenchyma. This finding is fully consistent with previous reports documenting parenchymal responses to an aerosolized MCh challenge, in which the separation of airway and tissue properties was accomplished by alveolar capsules (18, 21, 22, 27).

Reasons for Different Patterns With iv and Aerosol Challenge

A possible explanation for the different patterns of response of the lung, depending on the route of delivery, is that MCh acts on different structures when delivered by inhalation or iv. MCh produces a muscle contraction by stimulating the muscarinic cholinergic receptors (2). Sly et al. (25) investigated the role of the muscarinic receptors in puppies and reported that different receptors may be involved in producing airway and parenchymal constriction to inhaled MCh. M_3 receptors located on the airway smooth muscle, which are likely to be responsible for airway responses, may be more easily reached by iv-delivered MCh, whereas MCh delivered by aerosol has to diffuse across the respiratory epithe-

lium before reaching the muscle. On the other hand, M_1 receptors in the alveolar wall, which were reported to be involved in the parenchymal response (25), are likely to be reached more easily by aerosol delivery than by iv delivery. Under this scenario, it may be expected that an MCh infusion, delivered preferentially to the airway smooth muscle, will produce primarily airway constriction, whereas aerosolized MCh, delivered to the alveoli, will increase the tissue elastic and dissipative properties, as well as increasing Raw if the delivered dose is high enough. Several studies, performed in various species, have reported that the pulmonary tissues are more sensitive than the airways to aerosolized MCh (18, 27). Because the presence and the location of the muscarinic subtype receptors have been shown to be species dependent (2), this mechanism may also explain the apparent species difference in the MCh responsiveness of the airways and the parenchyma.

In an attempt to examine the mechanisms that give rise to an increase in Rti during MCh challenge, Nagase et al. (18) partitioned the response of the airways and the parenchyma after iv and aerosol administration of the agent by using alveolar capsules. They hypothesized that direct administration of the contractile agonist into the circulation should stimulate both the airway and parenchymal compartments homogeneously, whereas aerosol delivery would be likely to result in a heterogeneous airway response. Presenting histological evidence, they interpreted the higher increase in Rti after aerosol challenge as being due to the excessive tissue distortion, induced by heterogeneous constriction of the peripheral airways. However, in contrast to our result, they found a significant increase in the parenchymal elastance after MCh infusion. Another possible interpretation of our results is that MCh induced solely airway responses, regardless of the route of delivery. After an aerosol challenge, the uneven distribution of the particles around the bronchial tree could induce a heterogeneous peripheral airway response. This mechanism has been shown to generate a significant tissue distortion, i.e., the more sensitive regions or those regions to which the delivery is greater can be extremely constricted or even atelectatic, whereas adjacent regions can be hyperinflated (18). Obviously, this regional diversity after an aerosol challenge may significantly influence the estimation of the parenchymal mechanics by alveolar capsules because the sampling of the alveolar region is highly nonrepresentative and limited to subpleural areas. Should it occur to a significant degree, this phenomenon may also bias our parenchymal parameters, measured from the airway opening, in the following manner. The development of atelectatic regions may decrease the effective lung volume, resulting in increases in both Rti and EL (1). Additionally, hyperinflated regions adjacent to atelectatic areas can shift the operating volume of the working parenchyma toward its maximal volume, which would further increase the overall Rti and EL (1, 10, 28). The above analysis indicates that the apparent tissue constriction observed after aerosolized MCh could be produced by the excessive parenchymal distortion induced by an inhomogenous response of the peripheral airways, especially at extreme levels of constriction (that were probably not reached in the present investigations).

In summary, the results of the present study have demonstrated that airway and parenchymal responses to MCh in the rat can be partitioned on the basis of low-frequency ZL data. The changing pattern of the airway and tissue parameters indicates that the predominant site of action of MCh depends on the route of delivery. An iv MCh infusion induced purely airway constriction, whereas aerosolized MCh administration gave rise to constriction both in the airways and in the parenchyma. Although it is possible that the latter effects could be produced by a highly inhomogeneous constriction of the peripheral airways that led to a loss in lung volume, true differences in airway and tissue responses to MCh, possibly acting via different receptors, also seem very likely.

This study was supported by National Health and Medical Research Council of Australia Grant 960167 and the Hungarian Basic Research Fund (OTKA T016308).

Address for reprint requests: Z. Hantos, Dept. of Medical Informatics and Engineering, Albert Szent-Györgyi Medical Univ., PO Box 2009, H-6701 Szeged, Hungary.

Received 16 August 1996; accepted in final form 15 January 1997.

REFERENCES

1. **Barnas, G. M., and J. Sprung.** Effect of mean airway pressure and tidal volume on lung and chest wall mechanics in the dog. *J. Appl. Physiol.* 74: 2286–2293, 1993.
2. **Barnes, P. J.** Muscarinic receptor subtypes in airways. *Eur. Respir. J.* 6: 328–331, 1993.
3. **Bates, J. H. T., A.-M. Lauzon, G. S. Dechman, G. N. Maksym, and T. F. Schuessler.** Temporal dynamics of pulmonary response to intravenous histamine in dogs: effect of dose and lung volume. *J. Appl. Physiol.* 76: 616–626, 1994.
4. **Franken, H., J. Clément, M. Cauberghs, and K. P. Van de Woestijne.** Oscillating flow of a viscous compressible fluid through a rigid tube: a theoretical model. *IEEE Trans. Biomed. Eng.* 28: 416–420, 1981.
5. **Fredberg, J. J., D. Bunk, E. Ingenito, and S. A. Shore.** Tissue resistance and the contractile state of the lung parenchyma. *J. Appl. Physiol.* 74: 1387–1397, 1993.
6. **Fredberg, J. J., D. H. Keefe, G. M. Glass, R. G. Castile, and I. D. Frantz III.** Alveolar pressure nonhomogeneity during small-amplitude high-frequency oscillation. *J. Appl. Physiol.* 57: 788–800, 1984.
7. **Fredberg, J. J., and D. Stamenovic.** On the imperfect elasticity of lung tissue. *J. Appl. Physiol.* 67: 2408–2419, 1989.
8. **Hantos, Z., A. Adamicza, E. Govaerts, and B. Daróczy.** Mechanical impedances of lungs and chest wall in the cat. *J. Appl. Physiol.* 73: 427–433, 1992.
9. **Hantos, Z., B. Daróczy, T. Csendes, B. Suki, and S. Nagy.** Low-frequency mechanical impedance in the rat. *J. Appl. Physiol.* 63: 36–43, 1987.
10. **Hantos, Z., B. Daróczy, T. Csendes, B. Suki, and S. Nagy.** Modeling of low-frequency pulmonary impedance in dogs. *J. Appl. Physiol.* 68: 849–860, 1990.
11. **Hantos, Z., B. Daróczy, B. Suki, S. Nagy, and J. J. Fredberg.** Input impedance and peripheral inhomogeneity of dog lungs. *J. Appl. Physiol.* 72: 168–178, 1992.
12. **Hantos, Z., F. Peták, A. Adamicza, B. Daróczy, and J. J. Fredberg.** Histamine-induced constriction of the dog lung: differential responses of global airway, terminal airway, and tissue impedances. *J. Appl. Physiol.* 79: 1440–1448, 1995.
13. **Ingenito, E. P., B. Davison, and J. J. Fredberg.** Tissue resistance in the guinea pig at baseline and during methacholine constriction. *J. Appl. Physiol.* 75: 2541–2548, 1993.

14. **Kariya, S. T., L. M. Thompson, E. P. Ingenito, and R. H. Ingram, Jr.** Effect of lung volume, volume history, and methacholine on lung tissue viscance. *J. Appl. Physiol.* 66: 977–982, 1989.
15. **Lutchen, K. R., Z. Hantos, F. Peták, Á. Adamicza, and B. Suki.** Airway inhomogeneities contribute to apparent lung tissue mechanics during constriction. *J. Appl. Physiol.* 80: 1841–1849, 1996.
16. **Lutchen, K. R., B. Suki, D. W. Kaczka, Q. Zhang, Z. Hantos, B. Daróczy, and F. Peták.** Direct use of mechanical ventilation to measure respiratory mechanics associated with physiological breathing. *Eur. Respir. Rev.* 4: 198–202. 1994.
17. **Lutchen, K. R., B. Suki, Q. Zhang, F. Peták, B. Daróczy, and Z. Hantos.** Airway and tissue mechanics during physiological breathing and bronchoconstriction in dogs. *J. Appl. Physiol.* 77: 373–385, 1994.
18. **Nagase, T., A. Moretto, and M. S. Ludwig.** Airway and tissue behavior during induced constriction in rats: intravenous vs. aerosol administration. *J. Appl. Physiol.* 76: 830–838, 1994.
19. **Pellegrino, R., B. Violante, E. Crimi, and V. Brusasco.** Effects of aerosol methacholine and histamine on airways and lung parenchyma in healthy humans. *J. Appl. Physiol.* 74: 2681–2686, 1993.
20. **Peták, F., Z. Hantos, Á. Adamicza, and B. Daróczy.** Partitioning of pulmonary impedance: modeling vs. alveolar capsule approach. *J. Appl. Physiol.* 75: 513–521, 1993.
21. **Robatto, F. M., S. Simard, and M. S. Ludwig.** How changes in the serial distribution of bronchoconstriction affect lung mechanics. *J. Appl. Physiol.* 74: 2838–2847, 1993.
22. **Romero, P. V., F. M. Robatto, S. Simard, and M. S. Ludwig.** Lung tissue behavior during methacholine challenge in vivo. *J. Appl. Physiol.* 73: 207–212, 1992.
23. **Salerno, F. G., A. Moretto, M. Dallaire, and M. S. Ludwig.** How mode of stimulus affects the relative contribution of elastance and hysteresivity to changes in lung tissue resistance. *J. Appl. Physiol.* 78: 282–287, 1995.
24. **Sato, J., B. Suki, B. L. K. Davey, and J. H. T. Bates.** Effect of methacholine on low-frequency mechanics of canine airways and lung tissue. *J. Appl. Physiol.* 75: 55–62, 1993.
25. **Sly, P. D., K. E. Willet, S. Kano, C. J. Lanteri, and J. Wale.** Pirenzepine blunts the pulmonary parenchymal response to inhaled methacholine. *Pulm. Pharmacol.* 8: 123–129, 1995.
26. **Sly, P. D., and C. J. Lanteri.** Differential response of the airways and pulmonary tissues to inhaled histamine in young dogs. *J. Appl. Physiol.* 68: 1562–1567, 1990.
27. **Sly, P. D., and C. J. Lanteri.** Partitioning of the pulmonary response to inhaled methacholine in puppies. *J. Appl. Physiol.* 71: 886–891, 1991.
28. **Suki, B., F. Peták, Á. Adamicza, Z. Hantos, and K. R. Lutchen.** Partitioning of airway and lung tissue properties from lung input impedance: comparison of in situ and open chest conditions. *J. Appl. Physiol.* 79: 861–869, 1995.
29. **Van de Woestijne, K. P., H. Franken, M. Cauberghs, F. J. Landser, and J. Clement.** A modification of the forced oscillation technique. In: *Advances in Physiological Sciences. Respiration. Proc. of 28th Int. Cong. of Physiol. Sci. Budapest Hungary, June 1980*, edited by I. Hutás and L. A. Debreczeni. Oxford, UK: Pergamon, 1981, vol. 10, p. 655–660.

III

Eur Respir J 1999; 13: 767–774
Printed in UK – all rights reserved

European Respiratory Journal
ISSN 0903-1936

Effects of endothelin-1 on airway and parenchymal mechanics in guinea-pigs

Á. Adamicza*, F. Peták[†], T. Asztalos[†], Z. Hantos[†]

Effects of endothelin-1 on airway and parenchymal mechanics in guinea-pigs. Á. Adamicza, F. Peták, T. Asztalos, Z. Hantos. ©ERS Journals Ltd 1999.

ABSTRACT: The contributions of the airways and the parenchyma to the overall lung mechanical response to endothelin-1 (ET-1) have not been systematically studied. In this investigation, the ET-1 induced changes on lung mechanics in guinea-pigs were separated into airway and parenchymal components.

Pulmonary impedance (Z_L) data were collected between 0.5 and 21 Hz in six anaesthetized, paralysed, open-chest animals by introducing small-amplitude pseudorandom oscillations into the trachea through a wave tube. Z_L was calculated before and following intravenous boluses of ET-1, with doses doubled from 0.125–2 μg·kg of body weight^{-1}. A model containing an airway resistance (R_{aw}) and inertance (I_{aw}) and tissue damping (G) and elastance (H) was fitted to the Z_L spectra in each condition. Parenchymal hysteresis (η) was calculated as G/H.

After each dose, ET-1 induced significant increases in R_{aw} (at peak response mean±SEM: 424±129%), G (400±80%), H (95±22%) and η (156±33%), whereas I_{aw} decreased following the two highest doses (-291±77%).

These data suggest that the parenchymal constriction was accompanied by inhomogeneous constriction of the peripheral airways.

Eur Respir J 1999; 13: 767–774.

*Institute of Experimental Surgery and [†]Dept of Medical Informatics and Engineering, Albert Szent Györgyi Medical University, Szeged, Hungary.

Correspondence: Z. Hantos, Dept of Medical Informatics and Engineering, Albert Szent-Györgyi Medical University, H-6701 Szeged, P.O. Box 2009, Hungary. Fax: 36 62454566

Keywords: Airway resistance, bronchoconstriction, lung elastance, lung impedance, parenchymal resistance

Received: July 29 1998
Accepted after revision December 7 1998

This study was supported by Hungarian OTKA grants T016308, T016889 and T023089.

Endothelin-1 (ET-1) was originally described as a potent smooth muscle constrictor derived from vascular endothelial cells [1]. Numerous subsequent studies on the synthesis of ET-1 in nonvascular cell types, such as airway epithelial cells, type II pneumocytes and alveolar macrophages [2–4], have indicated the physiological and pathophysiological importance of this peptide in the lung. It is also known that ET-1 exerts a constrictor effect on both the vascular and the bronchial smooth muscles [5–11] However, the overall effect of ET-1 on lung mechanics has not been completely characterized.

Previous studies revealed dose-dependent increases in the peak pulmonary inflation pressure (PIP) [7, 9, 10], or elevations in the total lung resistance (R_L) with a concurrent decrease in the dynamic lung compliance (C_{dyn}) following the *i.v.* injection of ET-1 into guinea-pigs [5, 6, 8, 11]. The measurement of these global lung mechanical parameters, however, does not allow a separate estimation of the changes in the mechanical properties of the airways and parenchyma. Recent studies partitioning the lung responses to various constrictor agents into airway and parenchymal components established the importance of the elevated tissue resistance (R_{ti}) accompanying bronchoconstriction [12–20]. The only study on separation of the airway and parenchymal responses to ET-1 was reported by NAGASE *et al.* [16], who measured local alveolar pressures (P_A) through one or two alveolar capsules in guinea-pigs. It has been demonstrated, however, that PA exhibits a significant heterogeneity during constriction, which makes separations based on the measurement of PA highly accidental [12, 21]. Further, recent studies involving a model-based evaluation of lung impedance (Z_L) revealed that the parameters of a model of pulmonary mechanics estimated from low-frequency Z_L spectra characterize the airway and parenchymal mechanics accurately both in control conditions and during induced constrictions [12, 14, 15, 17, 19–23]. The aim of the present study, therefore, was to apply a model-based evaluation of Z_L data to investigate how ET-1 alters the separate mechanical properties of the airways and the parenchyma in guinea-pigs.

Methods

Animal preparation

Six Hartley guinea-pigs, weighing 470–560 g, were anaesthetized with pentobarbital sodium (30 mg·kg of body weight^{-1}, *i.p.*). The animals were placed in the supine position on a heating pad to maintain the body temperature at ~37°C. A catheter in the carotid artery was used to measure arterial blood pressure (BP) by a transducer (Statham P23Db; Statham Instruments, Hato Rey, Puerto Rico). A jugular vein was cannulated for drug administration. After tracheostomy, a plastic cannula (l=30 mm, ID=2 mm) was introduced into the distal end of the trachea. Paralysis was accomplished with pipecuronium bromide (0.2 mg·kg of body weight^{-1}) and the animal was ventilated by a Harvard small animal respirator (Harvard Apparatus, South Natick, MA, USA) with a tidal volume of 6 mL·kg of body weight^{-1} and respiratory frequency of 70 breaths·min^{-1}. After midline sternotomy, the ribs were

widely retracted and a positive end-expiratory pressure (PEEP) of 2.5 hPa was applied. Maintenance doses of anaesthetic (10 mg·kg of body weight^{-1}) and paralytic (0.05 mg·kg of body weight^{-1}) were given as needed.

At the end of the experiments, the lungs were excised from each guinea-pig challenged with ET-1, and the ratio of the wet weight to the dry weight of the lungs (WW/DW) was calculated to estimate the amount of pulmonary oedema. The WW/DW values obtained in the main study population were compared with those calculated from another group of untreated normal guinea-pigs (n=7).

Study protocol

The measurements of Z_L were made in the control conditions and following every *i.v.* bolus of ET-1 (Alexis Corp., Läufelfingen, Switzerland) by doubling the doses from 0.125–2 μg·kg of body weight^{-1}. Prior to each dose, 3–6 measurements were made to establish the baselines. Z_L was recorded 0.5, 1, 2, 4, 6 and 8 min after each ET-1 bolus. Before the control measurements, the lungs were hyperinflated by superimposing two inspirations to open the possible atelectatic areas.

Measurements of Z_L

The wave-tube technique [24] was applied to determine the Z_L spectra, as described in detail previously [19]. Briefly, a loudspeaker-in-box system and the tracheal cannula were connected through a polyethylene wave tube (l=105 cm, ID=2 mm) during apnoeic periods. Lateral pressures were sensed at both ends of the wave tube with ICS transducers (33NA002D; ICSensors, Milpitas, CA, USA). The mechanical ventilation was interrupted at end-expiration and a forcing signal was introduced into the trachea. The computer-generated small-amplitude pseudo-random signal contained 23 noninteger multiple frequency components between 0.5 and 21 Hz. The pressure signals were low-pass filtered (25 Hz, 5th-order Butterworth) and digitized at a sampling rate of 128 Hz by an analogue-to-digital board of an IBM-compatible computer. Fast Fourier transformation was used to calculate the pressure transfer function spectra from the 6-s recordings by using 4-s time windows and 97% overlapping. Z_L was computed as the load impedance of the wave tube by using the transmission line theory [24, 25].

Parameter estimation

A model containing an airway and a constant-phase tissue compartment [12, 22] was fitted to the Z_L data by minimizing the squared sum of weighted differences between the measured and the modelled impedance data (F). The airways were characterized by a frequency-independent airway resistance (R_{aw}) and inertance (I_{aw}), while the tissue compartment included parenchymal damping (G) and elastance (H). Parenchymal hysteresis [26] values (η) were calculated as G/H. Impedance data points corrupted by the heart rate and its harmonics were omitted from the model fit.

The Z_L curves obtained in each of the control conditions were ensemble-averaged. The Z_L data measured after each dose of ET-1 were fitted individually, and the parameter values obtained from the 0.5-min recording were selected to characterize the constrictor responses.

Statistical analysis

The parameter values are reported as means±SEM. Repeated-measures one-way analysis of variance on ranks with the Student–Newman–Keuls multiple comparison procedure was used to assess the effects of ET-1 on the airway and parenchymal parameters. Statistical significances were accepted at $p<0.05$.

Results

Table 1 summarizes the effects of ET-1 on the systemic BP for the guinea-pigs studied. In agreement with previous findings [5–7, 9–11], ET-1 caused marked and statistically significant increases in BP, which were always fully reversible.

The real (R_L) and the imaginary (X_L) parts of a representative baseline Z_L spectrum, together with the model fit, are shown in figure 1. The low variations in the Z_L data indicate the high reproducibility of the measurements: noticeable deviations can be observed only at those frequency points that coincided with the heart rate or its harmonics. Qualitatively, the sharp decrease in R_L in the low-frequency range is attributed to the viscous resistance of the parenchyma, while the plateau at higher frequencies represents the flow resistance of the airways. The elastic properties of the parenchyma are reflected in the quasi-hyperbolic increase in X_L in the low-frequency range. The zero crossing and the quasi-linear increase in X_L at higher frequencies demonstrate the increasing influence of the airway inertance. The model fitted the Z_L data very well, with no systematic fitting error.

Figure 2 illustrates the set of Z_L spectra obtained in the control conditions and following the administration of increasing doses of ET-1 in an animal, as real *versus* imaginary parts (Nyquist plots). The relationships between the R_L and X_L are notably linear in the control conditions and during the different levels of ET-1-induced constriction at low frequencies, consistent with the constant-phase behaviour of the parenchyma. Deviations from linearity occur at high frequencies as a result of the dominance of the airway properties: the plateaus in R_L and the increasing effect of the I_{aw} on X_L. Increasing

Table 1. – Effects of endothelin-1 on systemic blood pressure (BP)

Endothelin-1 dose μg·kg of body weight^{-1}	Change in BP %
0.125	14.2±2.5*
0.25	30.4±10.5*
0.5	43.3±16.4*
1	95.9±15.7*
2	184.4±14.2*

*: $p<0.05$.

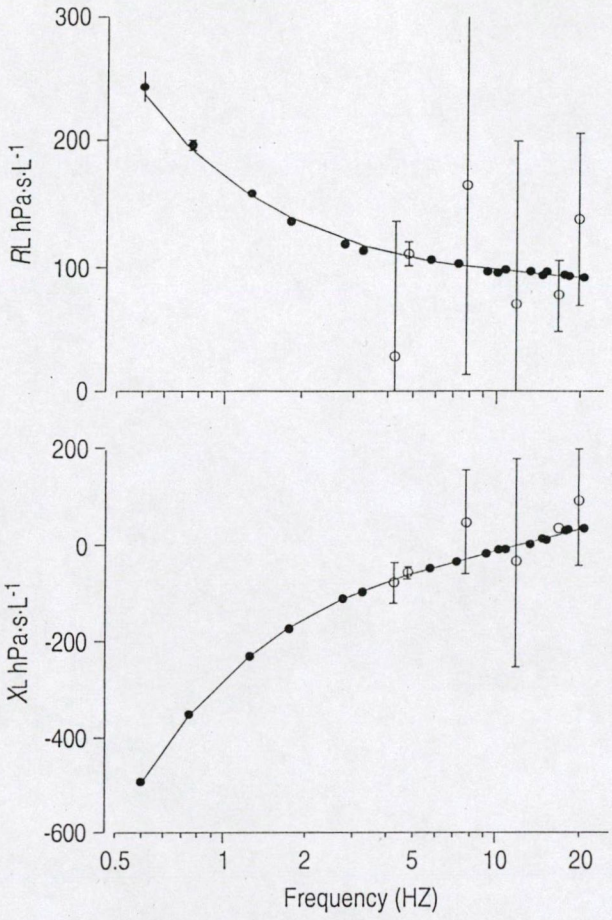

Fig. 1. – Real (R_L) and imaginary (X_L) parts of a representative pulmonary impedance spectrum obtained by averaging five successive measurements in the control condition (●) and the model fit (——). Data are mean±SEM. ○: data points corrupted by a cardiac artefact.

doses of ET-1 induced a monotonous increase in the high-frequency R_L, suggesting a marked airway response. However, the increases in R_L were consistently greater at low-frequencies, indicating dose-dependent increases in the parenchymal resistance. The elevations in the parenchymal elastance are reflected by the increases in the absolute values of the low-frequency X_L. The changing slopes of the X_L *versus* R_L relationships with increasing doses of ET-1 demonstrate a monotonous, dose-dependent increase in the parenchymal η. The constriction had no influence on the model performance: the differences between the measured and the modelled impedance data were small over the entire frequency range, independently of the lung condition. The baseline F (1.8±0.4%) was not significantly different from those obtained following the administrations of ET-1 (2.2±0.3%, 2.1±0.3%, 2.2±0.2%, 2.1±0.2% and 2.3±0.4% for the 0.125, 0.25, 0.5, 1 and 2 μg·kg of body weight^{-1} ET-1 bolus, respectively).

Temporal changes in the airway and tissue parameters during successive administrations of ET-1 doses obtained in an experiment are presented in figure 3. Increasing doses of the constrictor agent induced monotonous elevations in R_{aw}, G, H and η at low doses of ET-1, whereas no further increases in R_{aw} and H were observed when the concentration of the ET-1 dose was increased from 1 to 2 μg·kg of body weight^{-1}. All of the model parameters returned to

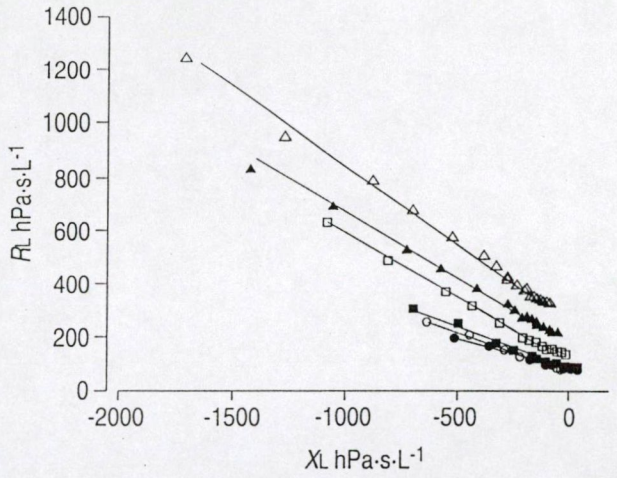

Fig. 2. – Real (R_L) *versus* imaginary (X_L) parts of pulmonary impedance data obtained in the control condition (●) and following endothelin-1 doses (○: 0.125; ■: 0.25; □: 0.5; ▲: 1; △: 2 μg·kg of body weight^{-1}). For the sake of simplicity, the impedance data points corrupted by a cardiac artefact have been omitted.

baseline following the low doses of ET-1; slight irreversible changes were seen only during severe constrictions. Peak responses occurred 30 s after administration of ET-1 in all model parameters when the constriction was moderate (following the three or four lowest doses), while the parameter increases were dissociated following the high doses of ET-1. Typically, G and η exhibited an instant peak increase after the injection of the bolus, whereas the peak response in H was slightly delayed. R_{aw} occasionally followed the changing pattern of G (*e.g.* after 1 μg·kg of body weight^{-1} in this example), or displayed a delayed increase (*e.g.* after 2 μg·kg of body weight^{-1}). Despite this asynchrony, the parameter values obtained 30 s after the ET-1 administrations adequately characterize the lung responses to most of the doses, although this sampling may lead to a slight underestimation of the increases in R_{aw} and H during severe constriction.

Figure 4 summarizes the airway and parenchymal parameters in control conditions and following increasing doses of ET-1 for the total group of animals. Monotonous and statistically significant elevations were obtained at all doses and in all of the parameters but I_{aw}, the decrease of which became significant only at higher ET-1 doses. Similar elevations occurred in R_{aw} and G, with maximal changes of 424±129% and 400±80% of the baseline values, respectively. The relative increases in H were far smaller, reaching a maximal value of 95±22%. Since the increases in G systematically exceeded those in H, statistically significant increases were obtained in η, which amounted to 156±33% following the highest ET-1 dose. These responses were more or less reversible: no residual effect of ET-1 was observed on I_{aw} or η, whereas high doses of ET-1 caused small but statistically significant, lasting increases in R_{aw} (37±10%), G (32±7%) and H (32±5%).

Relative changes in the mechanical parameters to increasing doses of ET-1 are demonstrated in figure 5. The percentage increases for each parameter were calculated by normalizing the responses to the corresponding

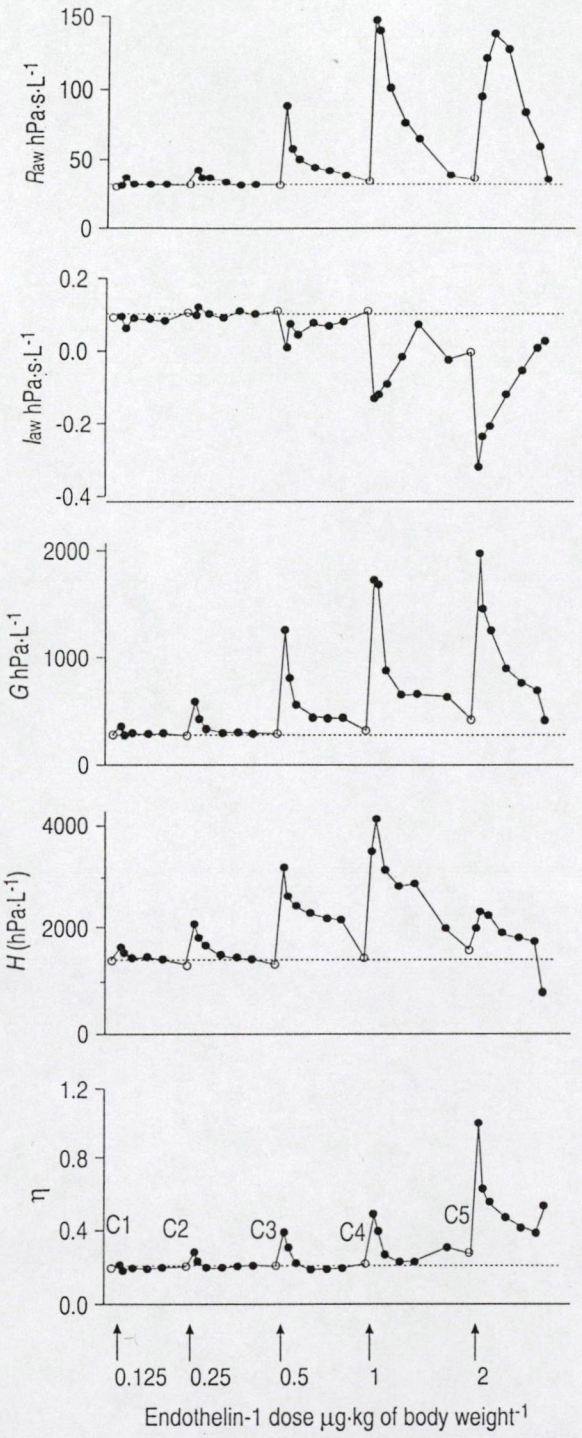

Fig. 3. – Airway and parenchymal parameters in control conditions (C1–C5; ○) and their temporal changes during increasing doses of endothelin-1 in a guinea-pig. *Raw*: airway resistance; *Iaw*: airway inertance; *G*: parenchymal damping; *H*: elastance; η: parenchymal hysteresis. - - - - : baseline.

baseline values preceding each ET-1 dose. The marked increases in *Raw* and *G* occurred reasonably in parallel, while the elevations in *H* and η were smaller. These increases were statistically significant following each ET-1 challenge except that in *Raw*, which remained at the baseline after the lowest dose of ET-1. No significant changes were found in *Iaw* after the lower doses of ET-1, whereas the last two doses of ET-1 induced marked and statistically significant decreases.

The ratios WW/DW in the untreated group were significantly lower (4.7±0.13) than those obtained from the ET-1-challenged guinea-pigs (5.2±0.14; $p<0.05$).

Discussion

The present study demonstrated that the airway responses to ET-1 were associated with significant changes in the mechanical properties of the lung parenchyma. Increasing concentrations of ET-1 induced progressive increases in *Raw* and monotonous increases in *G*, while *H* showed a plateau response at the three highest doses. In contrast, *Iaw* remained at the baseline level when the constrictions were mild, but exhibited significant decreases during severe constrictor responses. Although the changes in all mechanical parameters were fully reversible after the two lowest ET-1 doses, the higher doses caused irreversible parenchymal constrictions, which were associated with statistically significant residual increases in *Raw*. There were no changes in the baseline levels of *Iaw* or η.

To avoid the technical difficulties associated with the flow measurement in a small animal, in the present study the wave-tube technique was adopted to measure Z_L. Since this technique proved to afford reliable impedance data in rats [19], and the Z_L spectra in the present study are very similar to those obtained in previous studies in this similar-sized rodent [19], it was assumed that the Z_L curves accurately represent the mechanical impedance of the guinea-pig pulmonary system. Furthermore, in agreement with previous findings in other mammals [15, 17, 21, 23], the model involving an airway and a constant-phase tissue compartment was consistent with the frequency dependence of Z_L in guinea-pigs, resulting in no systematic fitting errors.

Airway responses

At low ET-1 doses, the dose-dependent increases in *Raw* were associated with no significant change in *Iaw*. For instance, at the ET-1 dose of 0.25 µg·kg of body weight^{-1} *Raw* doubled whereas *Iaw* remained at the control level (fig. 5). Since *Iaw* is thought to be a characteristic parameter of the central airways, this changing pattern suggests a dominance of the periphery in the development of an ET-1 induced airway constriction.

At high ET-1 doses, *Raw* exhibited further dose-dependent increases, while significant decreases occurred in *Iaw*, even negative values being attained in most of the animals during severe constriction. This seemingly controversial changing pattern in the airway parameters can be explained as follows. In the present study, the lumped parameters *Raw* and *Iaw* were used to characterize the mechanical properties of the overall bronchial tree. While both parameters are proportional to the overall length of the airways, *Iaw* and *Raw* are inversely related to the first and second power, respectively, of the overall bronchial cross-sectional area. Therefore, assuming no change in the overall airway length, both *Raw* and *Iaw* would be expected to increase with a generalized airway constriction. Although, in theory, *Raw* can increase while *Iaw* decreases if

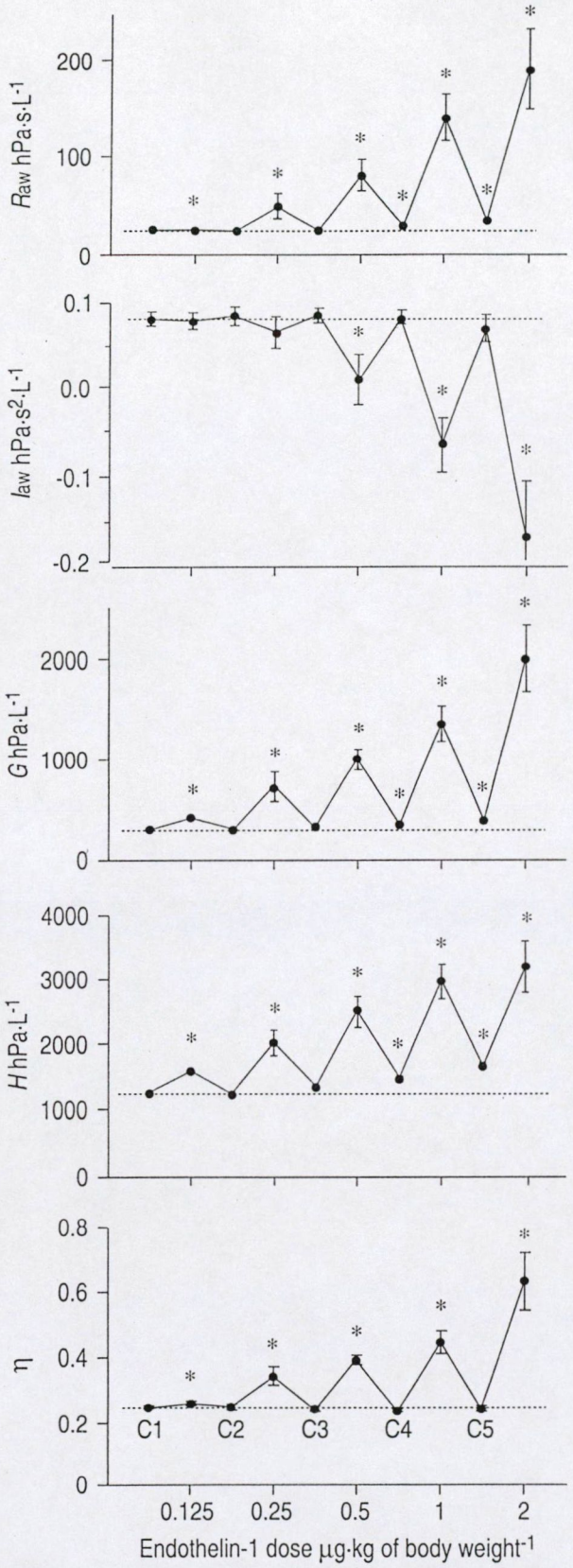

Fig. 4. – Airway and parenchymal parameters in control conditions (C1–C5) and their peak responses to endothelin-1 (0.125–2 µg·kg of body weight^{-1}) for the overall group of guinea-pigs. *: $p<0.05$ significant difference from the preceding control value. For definition see legend to figure 3. - - - - : baseline.

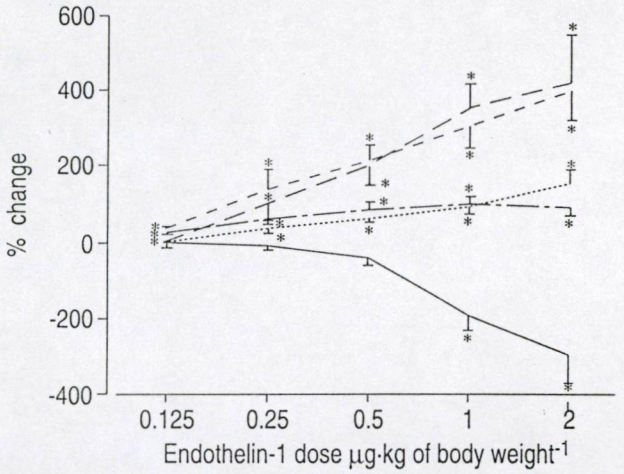

Fig. 5. – The effects of endothelin-1 on the values of the mechanical parameters. The responses in the parameters were normalized to the control values preceding each endothelin-1 dose — — : airway resistance; ——: airway intertance; – – –: tissue damping (G); — - —: elastance (H); · · · · · : G/H. *: $p<0.05$.

the airway constriction is associated with significant airway shortening, the unrealistic negative Iaw parameters obtained at high doses of ET-1 cannot be explained on that basis. Therefore, the opposite changes in Raw and Iaw during constriction can most probably be attributed to the failure of this simple lumped-parameter model during a severe spatial inhomogeneity of the pulmonary constriction. By using a distributed periphery lung model to simulate ZL data in control and constricted conditions, HANTOS *et al.* [12] demonstrated that, in the presence of an inhomogeneous peripheral constriction, the model-predicted Iaw systematically underestimates the real Iaw. Therefore, the opposite changes in Raw and Iaw at high ET-1 doses very probably indicate an inhomogeneous peripheral airway constriction.

Parenchymal responses

Significant increases in G and H parenchymal parameters during *i.v.* administrations of ET-1 were obtained. Since the elevations in G exceeded those in H, significant increases were obtained in η (fig. 5). In parenchymal strips obtained from guinea-pig lungs, FREDBERG *et al.* [27] demonstrated that different contractile agonists induced greater increases in the tissue resistance than in the elastance. Their data suggested that parenchymal constrictions were always associated with significant increases in the intrinsic η. Therefore, the constrictor responses in the present study can be interpreted in terms of ET-1 altering the coupling between the resistive and elastic properties at an elementary level of the parenchyma, *i.e.* ET-1 may induce significant elevations in the intrinsic η.

The constant-phase tissue model assumes that the entire frequency dependence of RL can be attributed to the resistive contribution of the parenchyma, while the quasi-hyperbolic increase in XL reflects lung tissue elasticity. Although this assumption seems to be valid in a relatively homogeneous healthy lung [15, 21], inhomogeneous peripheral airway constriction has been shown to increase the frequency dependence of RL [17, 19]. In this condition,

therefore, the parameter G may contain a significant artefactual component due to inhomogeneous peripheral ventilation [17]. Although the data do not allow an estimation of the roles of the intrinsic and artefactual increases in G separately, the pattern of changes in the mechanical parameters suggests that both phenomena may have been present: the finding that H exhibited marked and statistically significant increases in response to ET-1 suggests real parenchymal constrictions, which were probably associated with significant elevations in the intrinsic G, whereas the significant increase in G with no further increase in H at the highest dose of ET-1 can be attributed primarily to the enhanced peripheral inhomogeneity.

Residual effects

Although perfect returns to baseline were found for each parameter following low doses of ET-1, severe constrictions caused slight, but statistically significant residual elevations in R_{aw}, G and H. One possible explanation for such a change would be that the lung remained constricted after the severe ET-1-induced responses. In this case, however, the parameter η would also be expected to remain above the baseline level [27]. The slight systematic residual elevations in R_{aw}, G and H can therefore more probably be attributed to slight but irreversible restrictive changes in the lung *via* a permanent and progressive lung air volume loss. Since hyperinflations were performed between the ET-1 doses to recruit atelectatic alveolar regions, this loss in the lung air volume most probably resulted from pulmonary oedema [28]. The finding in the present study that the ratios WW/DW were significantly higher in guinea-pigs challenged with ET-1 supports this assumption. The possible presence of oedema is in agreement with the results of FILEP *et al.* [29], who observed increases in the vascular permeability after high doses of ET-1.

Airway and tissue responses to ET-1

Several authors have demonstrated a significant lung response to an *i.v.* injection of ET-1 by measuring PIP [7, 9, 10] or R_L and C_{dyn} [5, 6, 8, 11] as indicators of the constriction. However, PIP reflects the overall pressure losses in the lungs, and the value of R_L contains a flow resistive airway (R_{aw}) and a viscoelastic parenchymal tissue (R_{ti}) component. Accordingly, the methods used in these previous studies do not allow a detailed investigation of the effects of ET-1 on the lung mechanics. NAGASE and coworkers [16, 18] separated the ET-1-induced lung responses into airway and parenchymal components in guinea-pigs and in mice. In contrast to the present finding that the relative changes in the airway and parenchymal resistances were approximately equal, they reported an almost 3-times greater elevation in R_{ti} (340%) than that in R_{aw} (127%) following a 2.4 μg·kg of body weight^{-1} *i.v.* ET-1 bolus in guinea-pigs. Besides the substantial difference in the size of the guinea-pigs, methodological differences between the studies may explain this discrepancy, as follows. The baseline R_{aw} values obtained by NAGASE *et al.* [16] were about 4-times greater than those obtained in the present study, suggesting the inclusion of the resistance of the endotracheal tube in their R_{aw} values. This instrumental component of R_{aw} comprises a significant proportion of the total frequency-independent resistance, and this component does not change during constriction. The relative ET-1-induced R_{aw} increases reported by NAGASE *et al.* [16] may therefore have been underestimations, unlike those in the present study, where the airway responses were based on R_{aw} values excluding the resistance of the tracheal cannula. Moreover, NAGASE *et al.* [16] separated the airway and parenchymal responses by measuring the local P_A in open-chest guinea-pigs. It is obvious that the sampling of one or two alveolar regions in a highly inhomogeneously constricted lung [12, 15, 17, 19] makes the capsule-based partitioning highly incidental [21]. Furthermore, in an open-chest guinea-pig (and especially in the mouse [18]), where the outer diameter of the capsule is comparable to the entire sternocostal area of a lobe, the application of a capsule is very likely to influence the airway–tissue separation profoundly, in addition to the overall lung mechanics. The relatively large capsules fix a significant part of the lung surface, and hence may tend to uniformize the P_A distribution during constriction. This phenomenon may explain the striking observation by NAGASE *et al.* [16] that the differences in P_A of the two capsules were <10%, even during severe ET-1-induced constriction. Additionally, it appears that their finding of unusually low baseline η values (0.066) with a rather high coefficient of variation (67%) can also be attributed to uncertainties related to the P_A measurement in a small animal. In the present study, the mechanical properties of the airways and the parenchyma were separated in a far less invasive manner, by evaluating the input impedance data relating to the lungs.

Recent studies on separation of the lung response into airway and parenchymal components have established that constrictor agents, such as methacholine (MCh) [19], histamine [12, 15], prostaglandins [27] and ET-1 [16, 18], act on both the airway and tissue compartments. Although the differences in species and/or methodology may influence the pattern and the magnitude of the lung response, the constrictor agent and its delivery route seem to be the primary determinants of the shares of the airway and tissue compartments in the provoked constriction. For instance, in rats it was demonstrated that the two compartments participated about equally in the MCh-induced constriction when the agent was inhaled, whereas *i.v.* administered MCh predominantly caused an inhomogeneous airway constriction [19]. The airway responses to *i.v.* administered ET-1 in the present study were associated with significant increases in the parenchymal mechanics which is at odds to the MCh-induced lung responses. This finding suggests that different underlying mechanisms are involved in determining the constrictor responses of the lungs to MCh and ET-1.

Although it is generally accepted that the parenchyma contributes significantly to the constrictor response of the lungs, the mechanism of the altered lung tissue viscoelasticity is not completely clear. MITZNER *et al.* [30] presented experimental evidence that airway contraction could alter the parenchymal mechanics as a consequence of the mechanical interdependence between the airways and the lung tissues. Furthermore, since ET-1 has been shown to constrict the vascular smooth muscle [5–7, 9, 11], lung tissue distortions could also be generated by changes in the vascular smooth muscle tone. Finally, *in vitro* studies on

parenchymal strips, where the confounding influence of bronchial or vascular constriction in the tissue response is minimized, suggested that alterations occurred at the parenchymal level, although the increases in the tissue mechanics were much smaller than those observed for the whole lung [27]. The results of the present study do not allow a distinction between the individual effects of these mechanisms. Since ET-1-induced vascular constrictions are not associated with pulmonary vascular engorgement, it is suggested that an altered vasculature *per se* would not cause such significant (two-fold) increases in the parenchymal parameters. Furthermore, an analysis of the temporal changes in the airway and parenchymal responses to an ET-1 bolus allows an estimation of whether active parenchymal constriction occurred or whether only the indirect effects of the contracting conducting airways are reflected in the elevated G and H. The current study indicated distinctly different time courses in the responses of the mechanical parameters following a high dose of *i.v.* administered ET-1. Typically, in accordance with previous findings [20], the peak responses occurred first in G and η, while the maximal increases in R_{aw} and H were somewhat delayed. Accordingly, since a number of findings confirm that the airway and parenchymal constrictions in response to other bronchoactive agents are dissociated [13–15], active constriction of the parenchymal contractile elements in response to ET-1 can be suspected, but changes occurring in the lung tissue viscoelasticity as a result of parenchymal distortions might also have been involved when the lung constriction was fully developed.

In summary, it has been demonstrated that increasing doses of endothelin-1 affect the mechanical properties of the airways and the parenchyma in guinea-pigs in a dose-related manner. The dose-response curves for the airway and parenchymal mechanical parameters suggest the dominance of the peripheral airways in the development of the endothelin-1-induced constriction. Although a marked inhomogeneous constriction of the peripheral airways potentially biases an assessment of the changes in the lung tissue mechanics, intrinsic increases clearly occurred in the mechanical properties of the parenchyma. These results indicate that, besides the increases in tone in the vascular and bronchial smooth muscles, endothelin-1 also has a marked constrictor effect on the lung parenchyma.

Acknowledgements. The authors thank I. Kopasz and L.Vigh for excellent technical assistance

References

1. Yanagisawa M, Kurihara H, Kimura S, *et al.* A novel potent vasoconstrictor peptide produced by vascular endothelial cells. *Nature Lond* 1988; 332: 411–415.
2. Durham SK, Goller NL, Lynch JS, Fisher SM, Rose PM. Endothelin receptor B expression in the rat and rabbit lung as determined by *in situ* hybridization using nonisotopic probes. *J Cardiovasc Pharmacol* 1993; 22 (Suppl. 8): S1–S3.
3. Markewitz BA, Kohan DE, Michael JR. Endothelin-1 synthesis, receptors, and signal transduction in alveolar epithelium: evidence for an autocrine role. *Am J Physiol* 1995; 268: L192–L200.
4. Kobayashi Y, Sakamoto Y, Shibasaki M, Kimura I, Matsuo H. Human alveolar macrophages synthesize endothelins by thrombin. *J Immunol* 1997; 158: 5442–5447.
5. Macquin-Mavier I, Levame M, Istin N, Harf A. Mechanisms of endothelin-mediated bronchoconstriction in the guinea pig. *J Pharmacol Exp Therap* 1989; 250: 740–745.
6. Schumacher WA, Steinbacher TE, Allen GT, Ogletree ML. Role of thromboxane receptor activation in the bronchospastic response to endothelin. *Prostaglandins* 1990; 40: 71–79.
7. Pons F, Loquet I, Touvay C, *et al.* Comparison of the bronchopulmonary and pressor activities of endothelin isoforms ET-1, ET-2, and ET-3 and characterization of their binding sites in guinea pig lung. *Am Rev Respir Dis* 1991; 143: 294–300.
8. White SR, Darren DP, Tahtaway P, *et al.* Epithelial modulation of airway smooth muscle response to endothelin-1. *Am Rev Respir Dis* 1991; 144: 373–378.
9. Lueddeckens G, Bigl H, Sperling J, Becker K, Braquet P, Förster W. Importance of secondary TXA_2, release in mediating of endothelin-1 induced bronchoconstriction and vasopressin in the guinea-pig. *Prostagland Leuk Essent Fatty* 1993; 48: 261–263.
10. Noguchi K, Noguchi Y, Hirose H, *et al.* Role of endothelin ET_B receptors in bronchoconstrictor and vasoconstrictor responses in guinea-pigs. *Eur J Pharmacol* 1993; 233: 47–51.
11. Polakowski JS, Opgenorth TJ, Pollock DM. ET_A receptor blockade potentiates the bronchoconstrictor response to ET-1 in the guinea pig airway. *Biochem Biophys Res Comm* 1996; 225: 225–231.
12. Hantos Z, Daróczy B, Suki B, Nagy S, Fredberg JJ. Input impedance and peripheral inhomogeneity of dog lungs. *J Appl Physiol* 1992; 72: 168–178.
13. Bates JHT, Lauzon A-M, Dechman GS, Maksym GN, Schuessler TF. Temporal dynamics of pulmonary response to intravenous histamine in dogs: effect of dose and lung volume. *J Appl Physiol* 1994; 76: 616–626.
14. Lutchen KR, Suki B, Zhang Q, Peták F, Daróczy B, Hantos Z. Airway and tissue mechanics during physiological breathing and bronchoconstriction in dogs. *J Appl Physiol* 1994; 77: 373–385.
15. Hantos Z, Peták F, Adamicza Á, Daróczy B, Fredberg JJ. Differential responses of global airway, terminal airway, and tissue impedances to histamine. *J Appl Physiol* 1995; 79: 1440–1448.
16. Nagase T, Fukuchi Y, Matsui H, Aoki T, Matsuse T, Orimo H. *In vivo* effects of endothelin A- and B-receptor antagonists in guinea pigs. *Am J Physiol* 1995; 268: L846–L850.
17. Lutchen KR, Hantos Z, Peták F, Adamicza Á, Suki B. Airway inhomogeneities contribute to apparent lung tissue mechanics during constriction. *J Appl Physiol* 1996; 80: 1841–1849.
18. Nagase T, Matsui H, Aoki T, Ouchi Y, Fukuchi Y. Lung tissue behavior in the mouse during constriction induced by methacholine and endothelin-1. *J Appl Physiol* 1996; 81: 2373–2378.
19. Peták F, Hantos Z, Adamicza Á, Asztalos T, Sly PD. Methacholine-induced bronchoconstriction in rats: effects of intravenous *vs.* aerosol delivery. *J Appl Physiol* 1997; 82: 1479–1487.
20. Suki B, Peták F, Adamicza Á, Daróczy B, Lutchen KR,

Hantos Z. Airway and tissue constrictions are greater in closed than in open-chest conditions. *Respir Physiol* 1997; 108: 129–141.
21. Peták F, Hantos Z, Adamicza Á, Daróczy B. Partitioning of pulmonary impedance: modeling *vs.* alveolar capsule approach. *J Appl Physiol* 1993; 75: 513–521.
22. Hantos Z, Adamicza Á, Govaerts E, Daróczy B. Mechanical impedance of the lungs and chest wall in the cat. *J Appl Physiol* 1992; 73: 427–433.
23. Suki B, Peták F, Adamicza Á, Hantos Z, Lutchen KR. Partitioning of airway and lung tissue properties: comparison of *in situ* and open-chest conditions. *J Appl Physiol* 1995; 79: 861–869.
24. Van de Woestijne KP, Franken H, Cauberghs M, Landsr FJ, Clément J. A modification of the forced oscillation technique. *In:* Hutás I, Debreczeni LA, eds. Advances in Physiological Sciences. Respiration. Proceedings of the 28th International Congress of Physiological Sciences. Vol. 10. Oxford, Pergamon, 1981; pp. 655–660.
25. Franken H, Clément J, Cauberghs M, Van de Woestijne KP. Oscillating flow of a viscous compressible fluid through a rigid tube: a theoretical model. *IEEE Trans Biomed Eng* 1981; 28: 416–420.
26. Fredberg JJ, Stamenovic D. On the imperfect elasticity of lung tissue. *J Appl Physiol* 1989; 67: 2408–2419.
27. Fredberg JJ, Bunk D, Ingenito E, Shore SA. Tissue resistance and the contractile state of lung parenchyma. *J Appl Physiol* 1993; 74: 1387–1397.
28. Grossman RF, Jones JG, Murray JF. Effects of oleic acid-induced pulmonary edema on lung mechanics. *J Appl Physiol* 1980; 48: 1048–1051.
29. Filep JG, Fournier A, Földes-Filep E. Acute pro-inflammatory actions of endothelin-1 in the guinea-pig lung: involvement of ET_A and ET_B receptors. *Br J Pharmacol* 1995; 115: 227–236.
30. Mitzner W, Blosser S, Yager D, Wagner E. Effect of bronchial smooth muscle contraction on lung compliance. *J Appl Physiol* 1992; 72: 158–167.

IV

ENDOTHELIN-1-INDUCED AIRWAY AND PARENCHYMAL MECHANICAL RESPONSES IN GUINEA PIGS: THE ROLES OF ET_A AND ET_B RECEPTORS

Ágnes Adamicza[1], Ferenc Peták[2], Tibor Asztalos[2], László Tiszlavicz[3], Mihály Boros[1], Zoltán Hantos[2]

Institute of Surgical Research[1], Department of Medical Informatics and Engineering[2] and Department of Pathology[3], University of Szeged, Szeged, Hungary

Address for correspondence: Zoltán Hantos, Ph.D.
Department of Medical Informatics and Engineering
University of Szeged
H-6701 Szeged, P. O. Box 427, Hungary
Phone: +36 62 545 077
Fax: +36 62 544 566
E-mail: hantos@dmi.szote.u-szeged.hu

Running title: ET_A and ET_B receptors in lung mechanical responses

Keywords: Endothelin-1, Endothelin receptor antagonists, Lung impedance, Airway resistance, Parenchymal resistance, Lung elastance

Abstract

We have previously demonstrated the separate mechanical responses to increasing doses of endothelin-1 (ET-1) in the airways and parenchyma. In the present study, we have assessed the involvement of the ET_A and ET_B receptors in the ET-1-induced changes in lung mechanics.

A model-based evaluation of the low-frequency pulmonary impedance (ZL) was used to separate the airway and parenchymal responses in anaesthetized, paralysed, open-chest guinea pigs. A model containing an airway compartment and a constant-phase tissue compartment was fitted to the ZL spectra to estimate airway resistance (Raw) and inertance (Iaw) and tissue damping (G) and elastance (H). Parenchymal hysteresivity (η) was calculated as G/H.

Two successive doses of ET-1 (0.05 and 0.2 nmol/kg) each evoked significant dose-related increases in Raw, G, H and η. Pretreatment with 20 nmol/kg BQ-610 (an ET_A receptor antagonist) resulted in a significantly decreased elevation only in H after the lower dose of ET-1; however, all parameters changed significantly after pretreatment with 80 nmol/kg BQ-610, with 20 nmol/kg ETR-P1/fl (an ET_A receptor antagonist) or with 20 nmol/kg IRL 1038 (an ET_B receptor antagonist.

Our results demonstrate that ET-1 induces airway and parenchymal constriction via stimulation of both the ET_A and the ET_B receptors, and support the presence of a non-homogeneous ET_B receptor population in the guinea pig lung.

Introduction

Endothelin-1 (ET-1) is a powerful regulator of smooth muscle tone in many systems in both physiologic and pathophysiologic conditions. ET-1 induces vasoconstrictor and bronchoconstrictor responses [1, 4, 5, 6, 9, 10], which suggests that an upregulated ET-1 release may play an important role in a variety of pulmonary disorders, such as pulmonary hypertension or bronchial asthma. Vasoconstriction is mediated by the ET_A receptors, whereas the ET_B receptors mediate both vasoconstriction and vasodilation, depending on the species and the particular circulatory region [1]. In the airways, the ET_A and ET_B receptor types coexist [2, 3] and both are involved in ET-1-induced bronchoconstriction [4, 5]. In the guinea pig, the ET_B receptors predominate in the lung [3], and the proportion of ET_B is greater in the bronchi than in the trachea [2].

The bronchoconstrictor nature of ET-1 has been concluded from the global changes in the mechanical parameters of the lung [6-11]. However, the situation is confused by observations that pulmonary parenchymal tissues may also contribute to the mechanical alterations in the lung during bronchoconstriction [12-14], as demonstrated by recent studies involving a model-based evaluation of pulmonary impedance (ZL) [15-17].

In vivo evidence for ET-1-induced parenchymal changes is difficult to establish. Although Nagase et al. [5] observed that ET-1 may cause increases in airway and tissue resistance and tissue elastance in the guinea pig lung, the contribution of the parenchyma to the net effects has not been fully elucidated. These authors measured inhomogeneous local alveolar pressures, and it has been demonstrated that such sampling may not be representative of the global state, since the regional variability of isolated mechanical alterations cannot be excluded [15]. We have recently characterized the airway and parenchymal components separately with the ZL-assessment technique, and

demonstrated that increasing doses of ET-1 elicit dose-dependent increases in the airway and parenchymal parameters in guinea pigs [17].

The aim of the present study was to assess whether pretreatment with ET receptor antagonists would influence the particular pulmonary responses to two doses of exogenous ET-1. In our previous paper [17] we used increasing doses of ET-1, however, in the present study, two of the doses were chosen: 0.05 nmol/kg, which caused slight, but significant changes, and no inhomogeneity, and 0.2 nmol/kg, the dose that elicited significant changes in the airway inertance suggesting an inhomogeneous peripheral airway constriction. We employed BQ-610, a compound with specific ET_A receptor antagonist properties [18], ETR-P1/fl, likewise an ET_A receptor antagonist [19], and IRL 1038, a selective ET_B receptor antagonist [20].

Material and methods

Animal preparation. The study was approved by the University Ethical Committee for the Protection of Animals in Scientific Research and performed in adherence to the NIH guidelines on the use of experimental animals.

The experiments were carried out in guinea pigs (weighing 380-600 g) anaesthetized with pentobarbital sodium (30 mg/kg *i.p.*). The animals were placed on a heating pad to maintain body temperature at 37 °C. The right carotid artery and left jugular vein were cannulated for the measurement of mean arterial blood pressure (BP) and drug administration, respectively. A plastic cannula (length=30 mm, internal diameter=2 mm) was inserted into the trachea and connected to a small animal respirator (Harvard App. Inc., South Natick, MA, USA) delivering a tidal volume of 6 ml/kg at a frequency of 70/min. Following midline sternotomy, the chest was widely opened and a positive end-expiratory pressure of 2.5 cmH_2O was applied. The guinea pigs were paralysed with

pipecuronium bromide (0.2 mg/kg). Additional doses of pentobarbital sodium (10 mg/kg) and pipecuronium bromide (0.05 mg/kg) were given as needed to maintain anaesthesia and paralysis, respectively.

Experimental protocol. After the surgical procedure, the animals were allowed to stabilize for 20 min. They were then randomized to one of the five following groups and given *i.v.* ET-1 (Alexis Corp., Läufelfingen, Switzerland) in two successive doses, the first ET-1 dose at zero time (ET-1_1, 0.05 nmol/kg) and the second dose 10 min thereafter (ET-1_2, 0.2 nmol/kg) (group *ET-1*, n=9), or 20 nmol/kg ET_A receptor antagonist BQ 610 (Alexis Corp., Läufelfingen, Switzerland) (group *BQ-610*$_{20}$, n=8), or 80 nmol/kg ET_A receptor antagonist BQ-610 (group *BQ-610*$_{80}$, n=6), or 20 nmol/kg ET_B receptor antagonist IRL 1038 (Alexis Corp., Läufelfingen, Switzerland) (group *IRL 1038*, n=9), or and 20 nmol/kg ET_A receptor antagonist ETR-P1/fl (Kurabo Ltd., Osaka, Japan) (group *ETR-P1/fl*, n=5). The antagonist was administered 3 min prior to the first ET-1 dose (ET-1_1).

Pulmonary mechanics. Small-amplitude pseudorandom oscillations between 0.5 and 21 Hz were introduced into the trachea for 6-s intervals at end-expiration to determine the ZL spectra as previously described [16, 17]. Four measurements of ZL were made under the control conditions (before antagonist pretreatment and/or the administration of ET-1_1 and ET-1_2). Further ZL measurements were made at 0.5, 1, 2, 4 and 6 min after the administration of each of the successive ET-1 boluses. Prior to the control ZL measurements, the lungs were hyperinflated by occluding the expiratory line of the respirator for two consecutive cycles to prevent atelectasis. This manoeuvre was repeated at 7 min after each ET-1 dose. A model containing an airway and a constant-phase tissue compartment was fitted to the ZL data [15]; the airways were characterized by frequency-independent airway resistance (Raw) and inertance (Iaw), and the tissue properties were represented by parenchymal damping (G) and elastance (H).

Parenchymal hysteresivity (η) was calculated as G/H [21]. The control ZL spectra and those recorded after ET-1 antagonist administration were averaged separately and then fitted, whereas the ZL data obtained following the administration of the two successive doses of ET-1 were fitted individually. The constrictor responses to each of the ET-1 doses were characterized by the parameter values obtained from ZL recorded at 0.5 min after administration. Before the experiments, the resistance and inertance of the tracheal cannula were also measured, and were subtracted from the corresponding Raw and Iaw.

Gravimetric and morphometric analysis. At the end of each experiment, the animals were killed with an overdose of pentobarbital sodium, and lung tissue samples were taken for gravimetric and histological analysis. The wet weight of each sample (WW) was measured and the samples were then dried until a constant dry weight was reached (DW). The wet-to-dry ratio (WW/DW) for each sample was calculated. Histological analysis was also performed. Tissue samples of removed lungs for routine histology were fixed in 10 % neutral-buffered formalin and paraffin embedded. Sections of each sampled tissue were stained with H&E and PAS. We observed the alveoli (oedema fluid, polymorphonuclear cells, macrophages) and the alveolar capillaries (congestion).

Statistical analysis. The results are presented as means ± SE both for the absolute values and for the percentage changes from the control data. Non-parametric tests were used for statistical analysis. Friedman repeated measures analysis of variance on ranks with the Student-Newman-Keuls multiple comparison procedure, and Kruskal-Wallis one-way analysis of variance on ranks with the Dunn multiple comparison procedure, were used for within-group and between-group comparisons, respectively. A P value of < 0.05 was considered statistically significant.

Results

The resting BP values were not significantly different between the groups. In group *ET-1*, ET-1 induced significant dose-dependent increases in BP. The maximum values were reached within 1-2 min and BP then declined toward the baseline within 10 min. There were no significant differences in ET-1-induced BP changes between groups *BQ-610$_{20}$*, *IRL 1038* and *ET-1*, although ET-1$_2$ caused a somewhat smaller response in group *IRL 1038*. In groups *BQ-610$_{80}$* and *ETR-P1/fl*, the increase in BP was significantly less than that in group *ET-1* (data not shown).

Figure 1 presents the characteristic profiles of the changes in airway and parenchymal parameters after each of the two successive doses of ET-1, with and without pretreatment with the higher dose of BQ-610 or IRL 1038. There were only slight differences in baseline values between the individual groups; however, the control G value for group *BQ-610$_{20}$* was significantly different from that for group *ETR-P1/fl*. Both the first and the second doses of ET-1 induced significant increases in Raw, G, H and η in group *ET-1*, and this dose-dependent pattern remained in all groups which received antagonists. The parameters reached their maxima within 30 s after administration of either dose of ET-1, and the peak values then gradually declined toward the baseline. In group *BQ-610$_{20}$*, the elevations in respiratory parameters were close to those observed in group *ET-1*. However, in groups *BQ-610$_{80}$*, *IRL 1038* and *ETR-P1/fl*, each of the doses of ET-1 evoked significantly smaller increases in Raw, G, H and η. The patterns of change in Iaw were inconsequential: in all groups but group *BQ-610$_{20}$*, no statistically significant changes in Iaw were observed after either ET-1 dose.

In group *ET-1*, the durations of significant changes in Raw and H were dose-dependent. Significant changes in η persisted for 1 min, and those in G for 10 min after each of the ET-1 doses (Table 1). The lower dose of BQ-610 significantly shortened the

duration of changes in G, and increased those in η after ET-1_1. The responses in Raw, G and η were statistically significant only for short intervals in the cases of the higher dose of BQ-610, IRL 1038 and ETR-P1/fl.

Because of the high variations in the baseline data, the percentage changes in the airway (Raw) and parenchymal parameters (G, H and η) were calculated by normalizing the values measured at 30 s after each of the ET-1 doses to those obtained before ET-1 administration (Fig. 2). ET-1 induced dose-dependent increases in each of these parameters in group *ET-1*. In group *BQ-610*$_{20}$, the changes in most of the parameters did not differ significantly from the corresponding values in group *ET-1*; only the increase in H was significantly smaller after ET-1_1. The responses in Raw, G, H and η after each ET-1 dose were significantly smaller in groups *BQ-610*$_{80}$, *IRL 1038* and *ETR-P1/fl* as compared with those in group *ET-1*.

No significant differences in the counts of polymorphonuclear cells and macrophages between the groups were obtained; in addition, no signs of alveolar oedema were observed (data not shown). The absence of oedema was also supported by the results of gravimetric analysis of the tissue samples. The ratios WW/DW for all the antagonist-treated groups did not differ significantly from that for group *ET-1* (*ET-1* 5.11±0.1, *BQ-610*$_{20}$ 4.88±0.07, *BQ-610*$_{80}$ 5.63±0.2, *IRL 1038* 5.06±0.1 and *ETR-P1/fl* 5.19±0.1).

Discussion

This study confirms that exogenous ET-1 induces significant changes in the mechanical properties of the airways and parenchyma in the guinea pig lung, and that these changes are accompanied by increases in BP. Administration of ET_A and ET_B receptor antagonists alone did not change the basal values of the mechanical parameters, which suggests that endogenous ET-1 does not play a significant role in the regulation of

the resting bronchomotor tone in the guinea pig. However, each of the doses of ET-1 significantly increased Raw, G, H and η. The lower dose of BQ-610 significantly decreased the changes only in H after ET-1_1, whereas the higher dose of the antagonist also reduced those in Raw, G, and η. Pretreatment with IRL 1038 and ETR-P1/fl reduced the responses to ET-1 in both the airways and the parenchyma. Thus, it is concluded that ET-1 induces receptor-sensitive parenchymal reactions that are distinct from the airway responses.

ET-1 receptor antagonists. We used the selective ET_A receptor antagonist BQ-610, the ET_A receptor antagonist ETR-P1/fl and the selective ET_B receptor antagonist IRL 1038 to investigate the roles of the ET receptors in the mechanical properties of the airways and the parenchyma. BQ-610 is a highly selective ET_A receptor antagonist, being approximately 30000 times more effective inhibitor of ET_A than of ET_B receptors *in vitro* [18], and it effectively antagonizes the *in vivo* effects of ET-1 on the ET_A receptors [22, 23]. ETR-P1/fl is an "antisense-homology box"-derived peptide, which exhibits anti-ET_A receptor activity both *in vitro* [19] and *in vivo* [22, 23]. Additionally, it improves the symptoms and haemodynamic parameters in endotoxin shock [24] and in hypodynamic septic rats [23], and inhibits the endothelial cell-leukocyte interactions in response to ET-1 in the intestinal microcirculation in rats [22]. IRL 1038 binds specifically to the ET_B receptors in various mammalian tissues including the guinea pig lung [20].

Methodological view. Before a comparison of our results with other data in the literature, it is relevant to discuss certain aspects of the methodology. It has previously been demonstrated that *i.v.* ET-1 induces dose-dependent increases in the peak pulmonary inflation pressure [8-10] or elevations in total lung resistance and decreases in dynamic lung compliance [6, 7, 11]. However, it should be stressed that these parameters are indicators of the mechanical changes only in the global lung mechanics: the peak

inflation pressure combining the resistive and elastic responses and the total respiratory or pulmonary resistance combining the airway and tissue properties in a frequency-dependent manner. Our technique, involving a model-based evaluation of multiple-frequency ZL data, allows estimation of the parameters that characterize the airway and parenchymal mechanics separately, both under control conditions and during constrictions induced by drugs [15, 16, 25], including ET-1 [17]. In the latter study, the mechanical responses were similar at corresponding doses of ET-1. There are no data that are directly comparable with the present findings, and only one paper reports parenchymal changes induced by ET-1 in the guinea pig *in vivo* [5].

Airway and parenchymal responses. In our study, the two successive doses of ET-1 each caused significant dose-related changes in the mechanical properties of the airways and the parenchyma. Of the airway parameters, Raw was increased significantly, without any significant change in Iaw. Since Iaw is dominated by the inertance in the central airways, we conclude that ET-1 induces airway constriction in the periphery of the lung. IRL 1038, ETR-P1/fl and the higher dose of BQ-610 significantly decreased the elevation in Raw induced by each of the ET-1 doses.

Autoradiographic studies have demonstrated that ET_A and ET_B receptors coexist in the guinea pig lung, with an ET_A:ET_B receptor ratio of 1:4 [3]. Furthermore, Hay et al. [2] described regional differences in the distributions of the two ET receptor types in the airways. The primary bronchi contain more ET_B receptors, whereas the ET_A receptors predominate in the trachea. The relative contribution of the ET_B receptors to bronchoconstriction therefore increases in the distal direction along the respiratory tract [2]. Pharmacological investigations in isolated guinea pig bronchi provided evidence that ET-1 causes bronchoconstriction largely via ET_B receptor stimulation [4, 26]. Nagase et al. [5] found that both ET_A and ET_B receptor antagonists effectively reduce the ET-1-induced increases in airway resistance *in vivo*. In our experiments, IRL 1038, ETR-p1/fl

and the higher dose of BQ-610 significantly decreased the elevation in Raw after ET-1 administration. These data therefore indicate that both types of receptors are involved in the ET-1-induced increase in Raw.

We found that ET-1 produced significant elevations in the parenchymal parameters G, H and η, indicating substantial changes in the mechanical properties of the parenchyma. Pretreatment with IRL 1038, ETR-P1/fl and the higher dose of BQ-610 significantly diminished the responses in H after each of the ET-1 doses. Nagase et al. [5] reported that responses in tissue resistance and lung elastance to ET-1 did not differ significantly in the presence of BQ-123, whereas BQ-788 significantly decreased the responses in both tissue parameters. Battistini et al. [4] demonstrated that BQ-123 inhibited the ET-1-induced contraction in parenchymal strips *in vitro*; however, this treatment was ineffective in the bronchi. In our experiments, pretreatment with both doses of BQ-610, ETR-p1/fl or IRL 1038 significantly reduced the changes in H. These findings suggest that both types of ET receptors are involved in the mediation of ET-1-induced constriction in the parenchyma.

It has been proposed that a heterogeneous population of ET_B receptors exists in the guinea pig respiratory system [4, 9, 27]. In our experiments, pretreatment with BQ-610 in a dose of 20 nmol/kg had practically no effect on the ET-1-induced airway and parenchymal responses. However, pretreatment with the higher dose significantly decreased the changes in the airway and parenchymal parameters, suggesting that the higher concentration of ET_A antagonist resulted in the inhibition of both ET_A and ET_B receptors. The dose-dependent effect of the ET_A receptor antagonist BQ-610 on the ET-1-induced pulmonary constriction provides additional evidence for the hypothesis that there may be an ET_A receptor antagonist-binding ET_B receptor subtype in the guinea pig lung [4, 9, 27].

ETR-P1/fl peptide. Our study provides the first demonstration of the effects of the ET_A receptor antagonist ETR-P1/fl on the ET-1-induced mechanical changes in the lung. In the presence of ETR-P1/fl, significantly smaller elevations in Raw, G, H and η occurred after each dose of ET-1 than those observed in untreated animals. Moreover, the peptide decreased the durations of the significant changes in Raw, G and η after each ET-1 dose. Thus, ETR-P1/fl affected the pulmonary mechanics in the same dose as did IRL 1038, but not as BQ-610. Therefore, it is reasonable to suggest that ETR-P1/fl is not selective for ET_A receptors in the guinea pig lung. These findings, similarly to those of Szalay et al. [23], indicate that ETR-P1/fl may antagonize not only ET_A, but also ET_B receptors. Another explanation may be that ETR-P1/fl removes circulating ET-1, as was observed by Baranyi et al. [24] in dogs.

Circulatory responses. In agreement with previous findings [6-11, 28], our study established that the *i.v.* administration of ET-1 results in dose-related increases in BP in the guinea pig. The lower dose of BQ-610 and IRL 1038 had no effect on the ET-1-evoked changes in BP, whereas the higher dose of BQ-610 and the ET_A receptor antagonist ETR-P1/fl inhibited the increase in BP. These results demonstrate that the ET-1-induced BP increase is mediated mainly by ET_A receptors in the guinea pig.

Gravimetric and morphometric results. ET-1 has been shown to be a pro-inflammatory mediator. It induces intravascular leukocyte sequestration, and enhances albumin extravasation and oedema formation in the guinea pig lung [28]. Filep et al. [28] found that ET-1 in doses of 0.3 and 1 nmol/kg gives rise to albumin extravasation via activation of the ET_A receptors in the trachea and the bronchi, but not in the parenchyma. However, the present study shows that ET-1 doses of 0.05 and 0.2 nmol/kg do not elicit lung oedema, as evidenced by gravimetric and histological examinations. In agreement with these data, Macquin-Mavier et al. [6] did not observe significant lung oedema in

ET-1-treated animals. At present, an explanation cannot be given for these discordant results, and the dynamics of ET-1-induced oedema formation should be further investigated.

Secondary mediators. Several studies have established that various mediators can contribute to the mechanical changes induced by ET-1 in the lung. It has been demonstrated that the bronchoconstriction evoked by ET-1 could be mediated by thromboxane A_2 released via ET receptor activation [8, 29, 30]. Further, in the guinea pig lung ET-1 can release the bronchodilator prostacyclin [30] and nitric oxide [29]. The direct bronchoconstrictor effect of ET-1 can therefore be either potentiated or counteracted by secondary mediators.

In summary, we have characterized the pulmonary mechanical responses to the administration of ET-1, both with and without pretreatment with ET_A and ET_B receptor antagonists, with a method appropriate for the separate quantification of the airway and parenchymal components. The results reveal that the activation of both ET_A and ET_B receptor subtypes is involved in the mediation of the mechanical changes in response to ET-1 in the airways and the parenchyma. Since selective ET_A receptor antagonist treatment suppressed the changes in the mechanical responses in a dose-related manner, we suggest the existence of a heterogeneous ET_B receptor population in the guinea pig lung.

Acknowledgements. The authors are grateful to Drs Hidechika Okada and Lajos Baranyi for generous supply of the ETR-P1/fl peptide, and to Ágnes Fekete, Anna Nagyiván, István Kopasz and Lajos Vígh for their skilful technical assistance.

This study was supported by Hungarian OTKA grants T30670 and T023089.

References

1. Clozel M, Gray GA, Breu V, Löfflet BM, Osterwalder R. The endothelin ET-B receptor mediates both vasodilation and vasoconstriction *in vivo*. *Biochem Biophys Res Commun* 1992; 186: 867-873.

2. Hay DWP, Luttmann MA, Hubbard WC, Undem BJ. Endothelin receptor subtypes in human and guinea-pig pulmonary tissues. *Br J Pharmacol* 1993; 110: 1175-1183.

3. Goldie RG, D'Aprile AC, Self GJ, Rigby PJ, Henry PJ. The distribution and density of receptor subtypes for endothelin-1 in peripheral lung of the cat, guinea-pig and pig. *Br J Pharmacol* 1996; 117: 729-735.

4. Battistini B, Warner TD, Fournier A, Vane JR. Characterization of ET_B receptors mediating contractions induced by endothelin-1 or IRL 1620 in guinea-pig isolated airways: effects of BQ-123, FR139317 or PD 145065. *Br J Pharmacol* 1994; 111: 1009-1016.

5. Nagase T, Fukuchi Y, Matsui H, Aoki T, Matsuse T, Orimo H. In vivo effects of endothelin A- and B-receptor antagonists in guinea pigs. *Am J Physiol* 1995; 268: L846-L850.

6. Macquin-Mavier I, Levame M, Istin N, Harf A. Mechanisms of endothelin-mediated bronchoconstriction in the guinea pig. *J Pharmacol Exp Therap* 1989; 250: 740-745.

7. Schumacher WA, Steinbacher TE, Allen GT, Ogletree ML. Role of thromboxane receptor activation in the bronchospastic response to endothelin. *Prostaglandins* 1990; 40: 71-79.

8. Pons F, Loquet I, Touvay C, Roubert P, Chabrier P-E, Mencia-Huerta JM, Braquet P. Comparison of the bronchopulmonary and pressor activities of endothelin isoforms ET-1, ET-2, and ET-3 and characterization of their binding sites in guinea pig lung. *Am Rev Respir Dis* 1991; 143: 294-300.

9. Noguchi K, Noguchi Y, Hirose H, Nishikibe M, Ihara M, Ishikawa K, Yano M. Role of endothelin ET_B receptors in bronchoconstrictor and vasoconstrictor responses in guinea-pigs. *Eur J Pharmacol* 1993; 233: 47-51.

10. Lueddeckens G, Bigl H, Sperling J, Becker K, Braquet P, Förster W. Importance of secondary TxA_2 release in mediating of endothelin-1 induced bronchoconstriction and vasopressin in the guinea-pig. *Prostagland Leuk Essent Fatty* 1993; 48: 261-263.

11. Polakowski JS, Opgenorth TJ, Pollock DM. ET_A receptor blockade potentiates the bronchoconstrictor response to ET-1 in the guinea pig airway. *Biochem Biophys Res Comm* 1996; 225: 225-231.

12. Ludwig MS, Robatto FM, Simard S, Stamenovic D, Fredberg JJ. Lung tissue resistance during contractile stimulation: structural damping decomposition. *J Appl Physiol* 1992; 72: 1332-1337.

13. Ingenito EP, Davison B, Fredberg JJ. Tissue resistance in the guinea pig at baseline and during methacholine constriction. *J Appl Physiol* 1993; 75: 2541-2548.

14. Bates JHT, Lauzon A-M, Dechman GS, Maksym GN, Schuessler TF. Temporal dynamics of pulmonary response to intravenous histamine in dogs: effects of dose and lung volume. *J Appl Physiol* 1994; 76: 616-626.

15. Hantos Z, Daróczy B, Suki B, Nagy S, Fredberg JJ. Input impedance and peripheral inhomogeneity of dog lungs. *J Appl Physiol* 1992; 72: 168-178.

16. Peták F, Hantos Z, Adamicza Á, Asztalos T, Sly PD. Methacholine-induced bronchoconstriction in rats: effects of intravenous vs. aerosol delivery. *J Appl Physiol* 1997; 82: 1479-1487.

18. Ishikawa K, Fukami T, Nagase T, Mase T, Hayama T, Niiyama K, Fujita K, Urakawa Y, Kumagai U, Fukuroda T, Ihara M, Yano M. Endothelin antagonistic peptide derivatives with high selectivity for ET_A receptors. In: Schneider CH, Eberle AN, Eds. Peptides. Leiden, ESCOM Science Publishers, 1992; 685-686.

19. Baranyi L, Campbell W, Ohshima K, Fujimoto S, Boros M, Okada H. The antisense homology box: a new motive in proteins that codes biologically active peptides. *Nature Med* 1995; 9: 894-901.

20. Urade Y, Fujitani Y, Oda K, Watakabe T, Umemura I, Takai M, Okada T, Sakata K., Karaki H. An endothelin B receptor-selective antagonist: IRL 1038, [Cys^{11}-Cys^{15}]-endothelin-1(11-21). *FEBS* 1992; 311: 12-16.

21. Fredberg JJ, Stamenovic D. On the imperfect elasticity of lung tissue. *J Appl Physiol* 1989; 67: 2408-2419.

22. Boros M, Massberg S, Baranyi L, Okada H, Messmer K. Endothelin 1 induces leukocyte adhesion in submucosal venules of the rat small intestine. *Gastroenterology* 1998; 114: 103-114.

23. Szalay L, Kaszaki J, Nagy S, Boros M. The role of endothelin-1 in circulatory changes during hypodynamic sepsis in the rat. *Shock* 1998; 10: 123-128.

24. Baranyi L, Campbell W, Ohshima K, Fujimoto S, Boros M, Kaszaki J, Okada H. Antisense homology box-derived peptides represent a new class of endothelin receptor inhibitors. *Peptides* 1998; 19: 211-223.

25. Hantos Z, Peták F, Adamicza Á, Daróczy B, Fredberg JJ. Differential responses of global airway, terminal airway, and tissue impedances to histamine. *J Appl Physiol* 1995; 79: 1440-1448.

26. Hay DWP. Pharmacological evidence for distinct endothelin receptors in guinea-pig bronchus and aorta. *Br J Pharmacol* 1992; 106: 759-761.

27. Hay DWP, Luttmann MA. Nonpeptide endothelin receptor antagonists. IX. Characterization of endothelin receptors in guinea pig bronchus with SB 209670 and other endothelin receptor antagonists. *J Pharmacol Exp Therap* 1997; 280: 959-965.

28. Filep JG, Fournier A, Földes-Filep E. Acute pro-inflammatory actions of endothelin-1 in the guinea-pig lung: involvement of ET_A and ET_B receptors. *Br J Pharmacol* 1995; 115: 227-236.

29. Lewis K, Cadieux A, Rae GA, D'Orleans-Juste P. L-NAME potentiates endothelin-stimulated thromboxane release from guinea pig lung. *J Cardiovasc Pharmacol* 1998; 31: S109-S111.

30. De Nucci G, Thomas R, D'Orleans-Juste P, Antunes E, Walder C, Warner TD, Vane JR. Pressor effects of circulating endothelin are limited by its removal in the pulmonary circulation and by the release of prostacyclin and endothelium-derived relaxing factor. *Proc Natl Acad Sci USA* 1988; 85: 9797-9800.

FIGURE LEGENDS

Figure 1. Mean airway (Raw and Iaw) and tissue parameter (G, H and η) profiles induced by two successive doses of ET-1 (ET-1_1 and ET-1_2) with and without pretreatment with one or other of two ET receptor antagonists. ANT: BQ-610_{80} or IRL 1038.

Figure 2. Changes induced in the parameters Raw, G, H and η by two successive ET-1 doses (ET-1_1 and ET-1_2) with and without pretreatment with an ET receptor antagonist. The parameters were measured at 30 s after each ET-1 dose and are normalized to the control values measured before ET-1 administration. * Significant difference ($P < 0.05$) from the value for group *ET-1*.

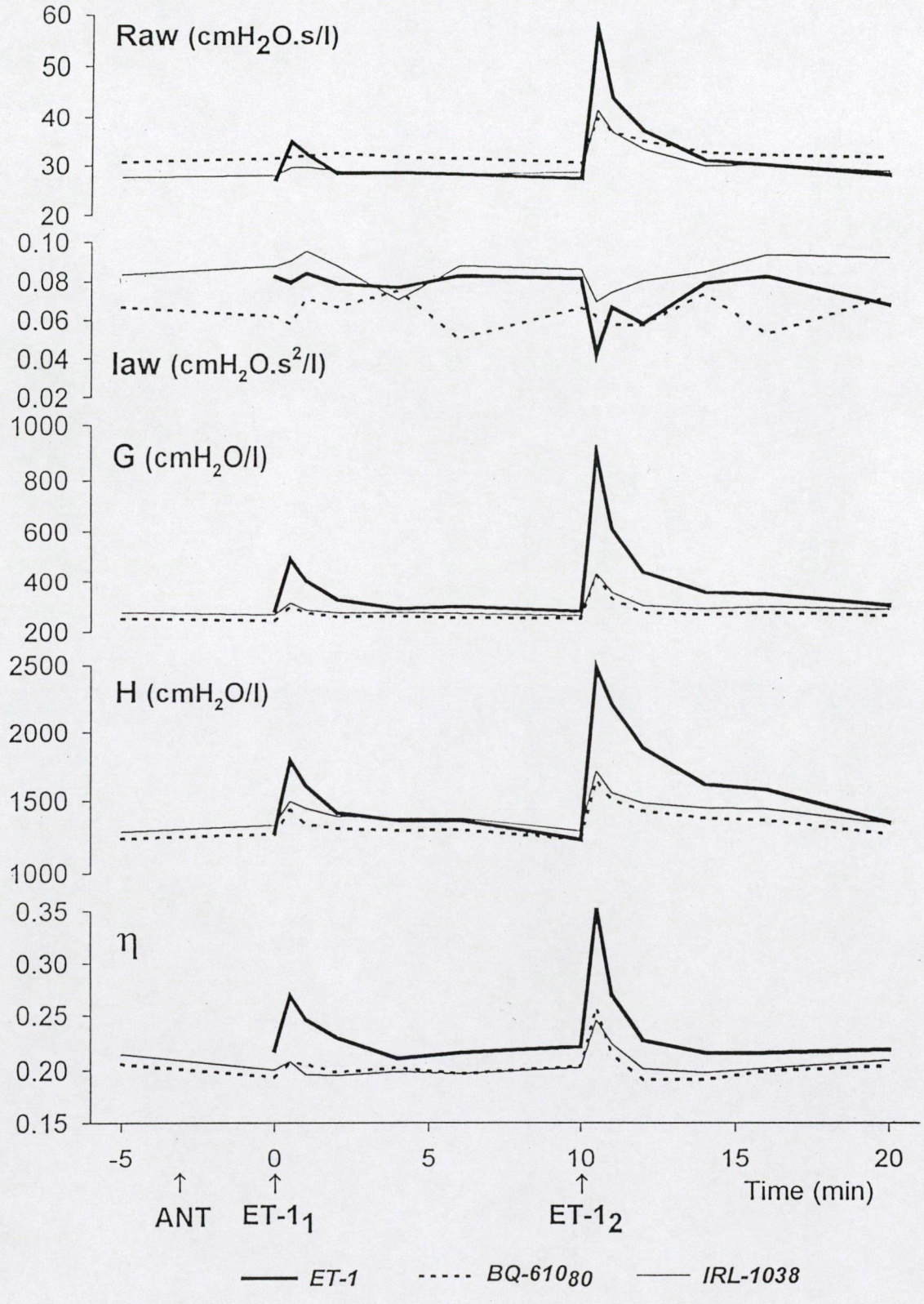
Raw (cmH2O.s/l)
60
50
40
30
20
0.10
0.08
0.06
0.04
0.02
Iaw (cmH2O.s2/l)
1000
800
600
400
200
G (cmH2O/l)
2500
2000
1500
1000
H (cmH2O/l)
0.35
0.30
0.25
0.20
0.15
η
-5
0
5
10
15
20
Time (min)
ANT
ET-11
ET-12
ET-1
BQ-61080
IRL-1038

Figure 1.

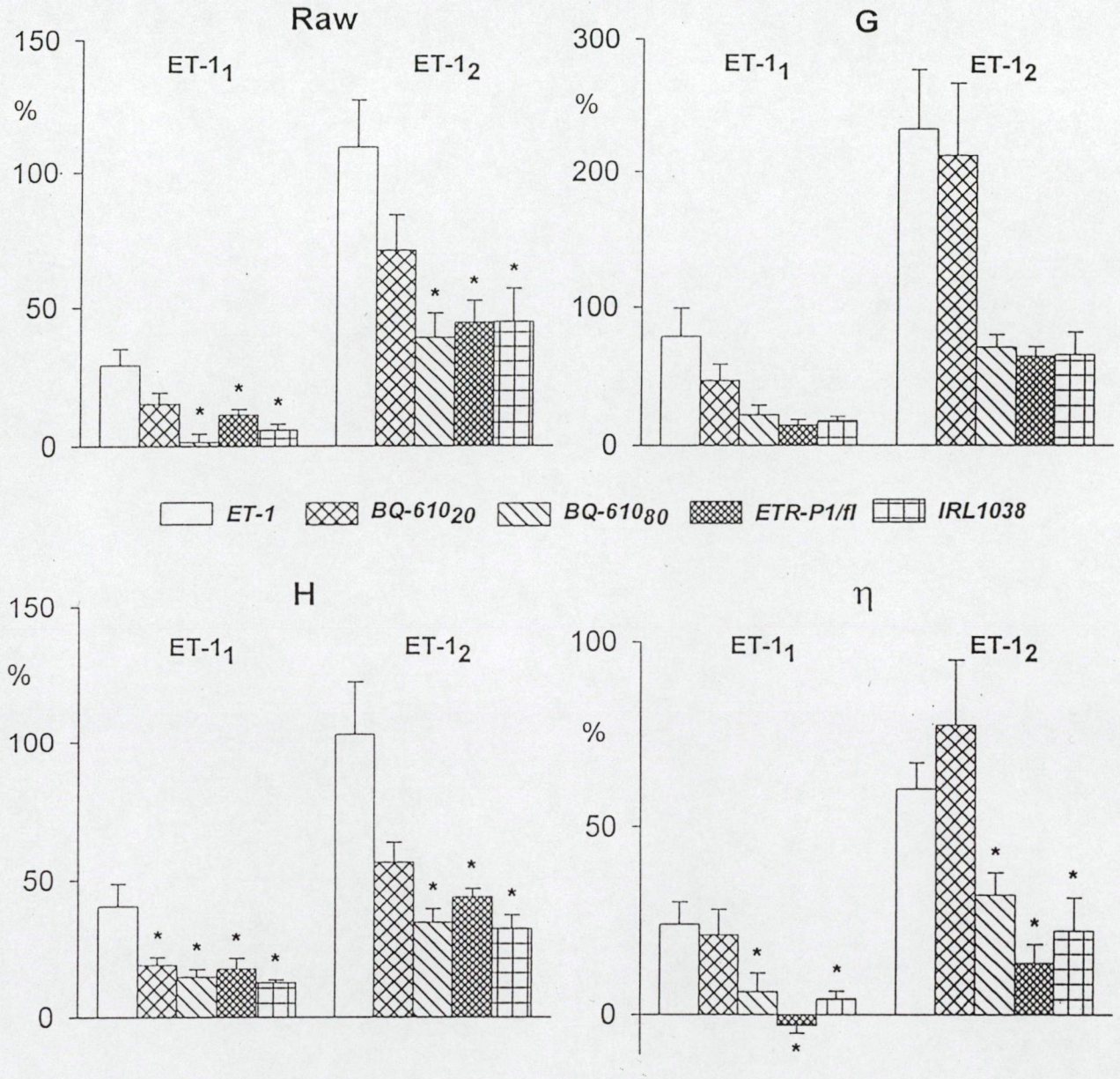
Raw
150
%
100
50
0
ET-1$_1$
ET-1$_2$
G
300
%
200
100
0
ET-1$_1$
ET-1$_2$
ET-1
BQ-610$_{20}$
BQ-610$_{80}$
ETR-P1/fl
IRL1038
H
150
%
100
50
0
ET-1$_1$
ET-1$_2$
η
100
%
50
0
ET-1$_1$
ET-1$_2$

Figure 2.

Table 1. Mean durations (min) of significant changes induced in airway (Raw) and parenchymal parameters (G, H and η) by two successive ET-1 doses ($ET\text{-}1_1$ and $ET\text{-}1_2$), with and without pretreatment with an ET-1 receptor antagonist.

Groups	Raw		G		H		η	
	$ET\text{-}1_1$	$ET\text{-}1_2$	$ET\text{-}1_1$	$ET\text{-}1_2$	$ET\text{-}1_1$	$ET\text{-}1_2$	$ET\text{-}1_1$	$ET\text{-}1_2$
ET-1	**1**	**6**	**10**	**10**	**6**	**10**	**1**	**1**
BQ-610$_{20}$	**6**	**4**	**1**	**6**	**6**	**10**	**4**	**1**
BQ-610$_{80}$	**0**	**0**	**0.5**	**1**	**1**	**6**	**0**	**0**
ETR-P1/fl	**0**	**2**	**0.5**	**1**	**10**	**6**	**0**	**0**
IRL 1038	**0**	**1**	**0.5**	**1**	**10**	**10**	**0**	**0**